JCTC Journal of Chemical Theory and Computation

Article

pubs.acs.org/JCTC

Cluster-Continuum Calculations of Hydration Free Energies of Anions and Group 12 Divalent Cations

Demian Riccardi,[†,‡] Hao-Bo Guo,[†] Jerry M. Parks,[†] Baohua Gu,[§] Liyuan Liang,[§] and Jeremy C. Smith*[,†,‡]

[†]UT/ORNL Center for Molecular Biophysics, Oak Ridge National Laboratory, 1 Bethel Valley Road, Oak Ridge, Tennessee 37831-6309, United States

[‡]Department of Biochemistry and Cellular and Molecular Biology, University of Tennessee, Knoxville, Tennessee 37996, United States

[§]Environmental Science Division, Oak Ridge National Laboratory, Oak Ridge, Tennessee 37831, United States

Supporting Information

ABSTRACT: Understanding aqueous phase processes involving group 12 metal cations is relevant to both environmental and biological sciences. Here, quantum chemical methods and polarizable continuum models are used to compute the hydration free energies of a series of divalent group 12 metal cations (Zn^{2+}, Cd^{2+}, and Hg^{2+}) together with Cu^{2+} and the anions OH^-, SH^-, Cl^-, and F^-. A cluster-continuum method is employed, in which gas-phase clusters of the ion and explicit solvent molecules are immersed in a dielectric continuum. Two approaches to define the size of the solute−water cluster are compared, in which the number of explicit waters used is either held constant or determined variationally as that of the most favorable hydration free energy. Results obtained with various polarizable continuum models are also presented. Each leg of the relevant thermodynamic cycle is analyzed in detail to determine how different terms contribute to the observed mean signed error (MSE) and the standard deviation of the error (STDEV) between theory and experiment. The use of a constant number of water molecules for each set of ions is found to lead to predicted relative trends that benefit from error cancellation. Overall, the best results are obtained with MP2 and the Solvent Model D polarizable continuum model (SMD), with eight explicit water molecules for anions and 10 for the metal cations, yielding a STDEV of 2.3 kcal mol^{-1} and MSE of 0.9 kcal mol^{-1} between theoretical and experimental hydration free energies, which range from −72.4 kcal mol^{-1} for SH^- to −505.9 kcal mol^{-1} for Cu^{2+}. Using B3PW91 with DFT-D3 dispersion corrections (B3PW91-D) and SMD yields a STDEV of 3.3 kcal mol^{-1} and MSE of 1.6 kcal mol^{-1}, to which adding MP2 corrections from smaller divalent metal cation water molecule clusters yields very good agreement with the full MP2 results. Using B3PW91-D and SMD, with two explicit water molecules for anions and six for divalent metal cations, also yields reasonable agreement with experimental values, due in part to fortuitous error cancellation associated with the metal cations. Overall, the results indicate that the careful application of quantum chemical cluster-continuum methods provides valuable insight into aqueous ionic processes that depend on both local and long-range electrostatic interactions with the solvent.

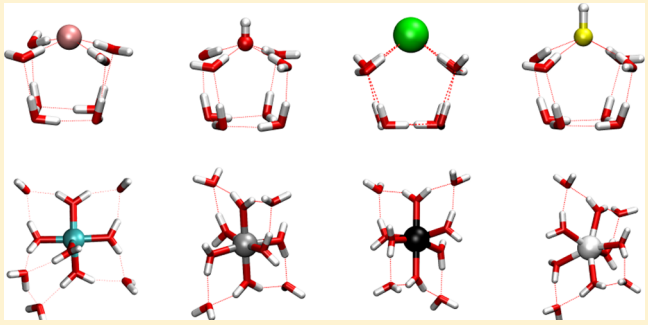

1. INTRODUCTION

Local and long-range electrostatic effects must be adequately described by any quantitative theoretical model of condensed phase processes. In principle, these effects can be treated with quantum-continuum models, which typically place the solute molecule of interest in a cavity within a dielectric medium.[1] The quantum mechanical charge distribution of the solute polarizes the continuum, which correspondingly exerts an electrostatic potential that influences the wave function of the solute; both may be solved iteratively[2] or directly during each self-consistent field cycle.[3] The geometry of the solute in the gas phase is commonly assumed to represent the geometry in the condensed phase.

Several quantum-continuum models have been developed that are able to reproduce hydration free energies to within ∼1 kcal mol^{-1} of experimental data for neutral species.[1,4,5] However, since continuum methods cannot accurately describe short-range intermolecular interactions such as hydrogen bonding, the inclusion of explicit, local water molecules is often necessary, e.g., in cluster-continuum studies of ion hydration free energies[6−18] and pK_a calculations.[19−23]

In previous cluster-continuum studies of ion hydration, the number of explicit water molecules has ranged from one[16] to that required for the hydration free energy to converge.[11,12,14,17] A high-level ab initio cluster-continuum study of the proton hydration free energy with minor contributions from concentration corrections[17] achieved excellent agreement

Received: April 10, 2012

   dx.doi.org/10.1021/ct300296k | J. Chem. Theory Comput. XXXX, XXX, XXX−XXX

Scheme 1. Thermodynamic Cycle for Computing Hydration Free Energies

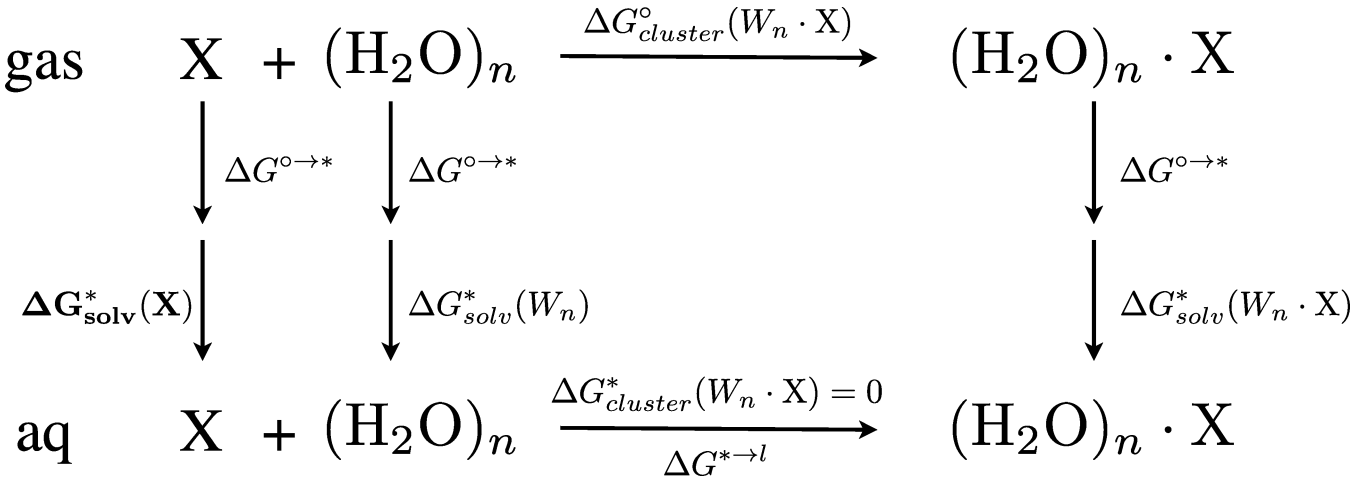

(within 0.5 kcal mol^{-1}) with the widely adopted experimental value of −265.9 kcal mol^{-1}[15,24−26] when only four explicit water molecules were included, agreeing to within 0.1 kcal mol^{-1} of that calculated with 10 water molecules.[11] Subsequent calculations using a similar approach were carried out for the hydration free energies of OH^-,[12] F^-,[14] and the solvated electron,[27] which is of central importance to condensed phase redox processes.[28] In a recent study employing density functional theory (DFT) cluster-continuum models, excellent agreement between theoretical and experimental hydration free energies was achieved for H^+ and Cu^{2+} by extrapolating from clusters as large as 14 and 18 molecules, respectively.[17] The calculated value for H^+ was only 0.8 kcal mol^{-1} more negative than the experimental value[24] of −265.9 kcal mol^{-1}, whereas Cu^{2+} was 3.1 kcal mol^{-1} more negative than the experimental value[25] of −505.9 kcal mol^{-1}. In contrast to the results from the high-level ab initio study,[11] the hydration free energy of H^+ became 4.6 kcal mol^{-1} more negative when the cluster size increased from four to 10.

Variational approaches have been employed to define the number of explicit water molecules using quasichemical calculations[9] and cluster-continuum approaches.[10] The variational cluster-continuum (VCC) method takes the number of explicit water molecules (n) as that for which the hydration free energy is the most favorable. As n increases from zero, regions of bulk continuum are exchanged for explicit solvent. Differences in the interactions among the solute and explicit water molecules or implicit solvent yields the n-dependence of the hydration free energy. Thus, the VCC approach provides a protocol for selecting the number of explicit water molecules to include. The original VCC study of 14 univalent ions (nine anions and five cations) achieved reasonable relative accuracy, with an average absolute error of 8.7 kcal mol^{-1} and a standard deviation of the average error of 2.9 kcal mol^{-1}, the latter increasing to ∼8 kcal mol^{-1} when no explicit water molecules were included.[10] The VCC approach is similar to the primitive approximation of quasichemical theory (QCT).[8,29] Defined within a statistical mechanics framework, QCT differs from VCC by maintaining a more restrictive definition of inner and outer regions that is more relevant to the condensed phase. That is, the inner region depends on the geometry of the solute[30] and is typically small enough to contain solvent molecules that interact *directly* with the solute. In contrast, cluster-continuum approaches such as VCC may include both directly and indirectly interacting (e.g., second hydration shell) water molecules.

In the present study, quantum chemical cluster-continuum methods are used to examine the hydration free energies of group 12 divalent metal cations (Zn^{2+}, Cd^{2+}, and Hg^{2+}) and a small set of anions (OH^-, SH^-, Cl^-, and F^-). SH^-, OH^-, and Cl^- anions are examined as they are relevant for group 12 metal−ligand binding in aquatic environments. We also include F^-, even though it interacts weakly with group 12 divalent metal cations in aqueous solution. Furthermore, the Cu^{2+} ion is also included for its intrinsic interest and to allow direct comparisons with previous cluster-continuum calculations.[17] These metals are a well characterized group that spans roles critical to enabling (Cu^{2+} and Zn^{2+}) and disrupting (Cd^{2+} and Hg^{2+}) biological function via environmental availability and contamination. However, the conclusions reached in this study are expected to be of interest for a wider range of ionic hydration processes.

The number of explicit water molecules needed is explored using two approaches. In the first approach, a constant number of water molecules (ranging from zero to six) is included, whereas in the second approach the number of water molecules is determined variationally. Following the results from high-level studies of OH^- and F^- hydration[12,14] and DFT studies of Cu^{2+} hydration,[17,31] the importance of the second hydration shell on relative and absolute hydration free energies is explored. The anion shells are expanded to include eight explicit water molecules, and the divalent metals are expanded to 10 explicit water molecules. Several related models for the polarizable continuum are compared in an effort to characterize model sensitivity for relative and absolute hydration free energy trends. Contributions to the hydration free energy are systematically analyzed to determine how each contribution is reflected in the absolute and relative errors between theory and experiment. Finally, recommendations are made for future studies of condensed phase anionic and cationic−metal hydration.

2. THEORETICAL BACKGROUND AND METHODS

2.1. Thermodynamic Cycle. Thermodynamic cycles for computing hydration free energies with cluster-continuum models have been discussed recently in detail[17] and are only briefly summarized here. The upper leg of the water cluster cycle (Scheme 1) involves gas-phase reactions between the

dx.doi.org/10.1021/ct300296k | J. Chem. Theory Comput. XXXX, XXX, XXX−XXX

solute, X, and *clusters* of water molecules (referred to as W_n or $(H_2O)_n$):

$$X + (H_2O)_n \rightleftharpoons X(H_2O)_n \quad (1)$$

Alternatively, the upper leg of the monomer cycle involves gas-phase reactions between the solute and n noninteracting water molecules

$$X + nH_2O \rightleftharpoons X(H_2O)_n \quad (2)$$

It has been shown that including intracluster water−water interactions on both sides of the reaction reduces the absolute error.[17] The hydration free energies, $\Delta G^*_{solv}(X)$, of the solute are calculated via Scheme 1 as

$$\Delta G^*_{solv}(X) = \Delta G^\circ_{cluster}(W_n{\cdot}X) + \Delta G^*_{solv}(W_n{\cdot}X) - \Delta G^*_{solv}(W_n) - \Delta G^{\circ\rightarrow *} - \Delta G^{*\rightarrow l} \quad (3)$$

which is the sum of the free energy of forming the gas phase solute−water cluster ($\Delta G^\circ_{cluster}(W_n{\cdot}X)$) with n explicit water molecules and the difference between the hydration free energies of the solute−water cluster ($\Delta G^*_{solv}(W_n{\cdot}X)$) and the water cluster, $\Delta G^*_{solv}(W_n)$. The standard state corrections adjust the gas phase concentrations ($\Delta G^{\circ\rightarrow *} = RT\ln(24.46)$) from 1 mol per 24.46 L to 1 M and the water cluster concentration from 1 M to 55.34/n M ($\Delta G^{*\rightarrow l} = RT\ln([H_2O]/n)$).[26,32] The gas-phase standard state correction ($\Delta G^{\circ\rightarrow *}$) is 1.89 kcal mol^{-1} at room temperature. The free energy change associated with exchanging the aqueous solute with the aqueous solute−solvent cluster (the aqueous $\Delta G^*_{cluster}(W_n{\cdot}X)$ in Scheme 1) is thermoneutral.[17,18] The term "microsolvation" is commonly invoked when a few water molecules are included in the absence of a continuum (e.g., refs 33 and 34), and we use it here accordingly when comparing the free energy of gas phase cluster formation ($\Delta G^\circ_{cluster}(W_n{\cdot}X)$) with experimental values. Recently, the above cycle was used to study the hydration of a large series of cations and anions with clusters containing five explicit water molecules[18] and also for the reference hydrated metal cation state in a study of metal binding specificity for the copper efflux regulator (CueR),[35] which used clusters of six water molecules for each metal ion: Ag^+, Cu^+, Au^+, Zn^{2+}, and Hg^{2+}.

In this study, the majority of hydration calculations are carried out using the water cluster cycle discussed above. The variationally determined hydration free energy is determined using the monomer cycle

$$\Delta G^*_{solv}(X) = \Delta G^\circ_{cluster}(W_n{\cdot}X) + \Delta G^*_{solv}(W_n{\cdot}X) - n\Delta G^*_{solv}(W_1) - n\Delta G^{\circ\rightarrow *} - nRT\ln([H_2O]) \quad (4)$$

where the n-scaled standard state contributions and hydration free energy of a single water molecule corresponds to formation of a solute−water molecule cluster from the solute and n noninteracting water molecules. Employing the monomer cycle describes hydration processes in terms of the change in interaction free energy as n single water molecules are transferred from solution to interact with the solute. As such, the treatment of the water molecules is simplified compared to Scheme 1. In terms of achieving quantitive agreement, the water cluster cycle benefits from error cancellation.[11,12,14,17] In terms of method development and validation, the monomer cycle provides useful information.

2.1.1. Free Energy Differences. When calculating relative hydration free energies between species X and Y using Scheme 1, the contributions from the standard state corrections ($\Delta G^{\circ\rightarrow *}$) cancel, i.e.,

$$\Delta\Delta G^*_{solv}(X, Y; n_x, n_y) = \Delta\Delta G^\circ_{cluster}(X, Y; n_x, n_y) + \Delta\Delta G^*_{solv}(X{\cdot}W_{n_x}, Y{\cdot}W_{n_y}) - \Delta\Delta G^*_{solv}(W_{n_x}, W_{n_y}) - RT\ln\frac{n_y}{n_x} \quad (5)$$

Furthermore, when the numbers of explicit water molecules are the same (i.e., $n_x = n_y$), the contributions from the hydration of the water cluster, $\Delta G^*_{solv}(W_n)$, and the corresponding concentration corrections also cancel, leaving only the differences between the gas-phase free energy for cluster formation and the associated cluster hydration free energy. Therefore, the relative trends in hydration calculated using the same number of explicit water molecules are independent of whether $(H_2O)_n$ or nH_2O is used in Scheme 1.

2.2. Comparing Theory and Experiment. Theoretical hydration free energies were compared to experimental values using the mean signed error (MSE) and the standard deviation of the average error (STDEV) to characterize both absolute and relative errors, respectively. Similar comparisons were carried out in the original VCC study.[10] Here, each error was calculated by subtracting the theoretical value from the experimental value, for which a negative error corresponds to underestimation because the experimental values are negative (all processes in the present study are favorable). For example, a large negative MSE paired with a small STDEV between experiment and theory corresponds to a systematic underestimation of the experimental values with reasonable relative accuracy. As another example, a set of calculated values that contains subsets (e.g., anions and divalent metal cations) that are internally consistent (small STDEVs) may yield a large STDEV for the entire set if the MSEs of the subsets are not sufficiently similar.

2.3. Computational Methods. All single-point energy calculations were carried out with Gaussian 09[36] using the B3PW91[37,38] or B3LYP[37,39,40] hybrid density functionals or second-order Møller−Plesset perturbation theory (MP2) with the frozen core approximation.[41] B3PW91[37,38] was chosen based on a recent, extensive study of group 12 dihalides.[42] B3PW91 has also been successfully used in previous studies of Hg^{2+} and Zn^{2+} coordination chemistry and exchange at model binding sites,[43] the microsolvation of Hg^{2+} complexes ($Hg(OH)_2$, Hg(OH)Cl, and $HgCl_2$),[44] and previous quantum chemical continuum calculations of the Hg−C bond cleavage reaction catalyzed by the organomercurial lyase MerB.[45] Besides widespread general use, B3LYP has been used recently in cluster-continuum studies of Cu^{2+} hydration,[17,31] QM/MM investigations of metal binding to CueR,[35] to model microsolvation effects (using two explicit water molecules) on interactions between group 12 divalent metal cations and cysteine,[34] and the microsolvation of mercury halide species.[33] B3PW91 and B3LYP were augmented with third-generation empirical dispersion corrections (i.e., DFT-D3) with Becke and Johnson damping and are referred to as B3PW91-D and B3LYP-D, respectively.[46,47]

On the basis of previous detailed studies,[11,12,14,48−50] MP2 with a sufficiently large basis set is expected to provide a more accurate description of gas-phase interactions than does density functional theory. Previous cluster continuum hydration calculations of UO_2^{2+} using 12 to 15 explicit water molecules

dx.doi.org/10.1021/ct300296k | J. Chem. Theory Comput. XXXX, XXX, XXX−XXX

found improvements using MP2 compared to DFT for describing the free energy difference (experimental value: -1.19 ± 0.42) between coordination numbers of four and five in solution.[49] Here, we focus on B3PW91-D and MP2 in the main text and include additional results for B3LYP in the Supporting Information.

Gas-phase contributions to the hydration free energies were computed using correlation-consistent basis sets, *aug*-cc-pVXZ, where X = D, T, or Q, which we abbreviate as *a*DZ, *a*TZ, and *a*QZ. For S and Cl, modified basis sets that include tight-*d* functions (i.e., *a*(X+*d*)Z) were used.[51] Basis sets[52] and corresponding pseudopotentials, abbreviated as *a*DZ-pp were used for Hg, Cu, Zn, and Cd.[53] We refer to a particular level of theory by the quantum chemical method, the basis set and pseudopotential used for the metal, and the basis set used for all other elements, for example, B3PW91-D/*a*TZ-pp/*a*TZ. For brevity, the use of the pseudopotential corresponding to the basis set is implied in the context of metal atoms, e.g., the last example becomes B3PW91-D/*a*TZ. The use of tight-d functions is implied for all molecules containing S or Cl.

MP2 energies at the estimated complete basis set limit (i.e., MP2/CBS) were computed as follows. The MP2 correlation energy was obtained using a two-point Halkier extrapolation[54] with the *a*TZ and *a*QZ basis sets. The correlation energy was then added to the unextrapolated HF/*a*QZ reference energy, because the gas-phase contributions to the hydration free energy at that level of theory were assumed to be essentially converged. For Cu^{2+}, unrestricted calculations were carried out.

Geometries of clusters with zero to six water molecules were optimized at the B3PW91/*a*DZ level of theory. Starting with configurations from the hydroxide hydration study in ref 12, geometry optimizations of OH^- and SH^- (hydroxide oxygen was replaced by sulfur) clustered with four and eight water molecules and the corresponding clusters of water molecules were optimized at the B3LYP/6-31++G(d,p) level with NWChem 6.0,[55] which is the same level of theory used in ref 12. Similarly, the starting configurations of F^- and Cl^- (fluoride was replaced by chloride) clustered with four and eight water molecules were taken from F^-–water clusters from ref 14. Additional geometry optimizations of the divalent metal cations clustered with 10 water molecules were optimized at the B3LYP/SDD/6-31+G(d,p) level using NWChem. For Zn^{2+}, Cd^{2+}, and Hg^{2+}, the 10 water molecule clusters were generated from a hexa-coordinated Cu^{2+} cluster determined in ref 31. Additional configurations of the divalent metal ions clustered with 10 water molecules were optimized with S4 symmetry constraints. The initial coordinates for the water clusters were taken from MP2 optimized geometries.[56,57]

All final geometries were optimized without symmetry constraints, and vibrational analyses were carried out to confirm minima and determine gas phase zero-point energy, thermal, and entropic contributions. The frequencies were scaled by 0.9646 and 0.9642 for B3PW91 and B3LYP, respectively, and all frequencies below 100 cm^{-1} were set to 100 cm^{-1} to reduce differences between functionals and artifacts due to anharmonicity.[23,58−60] For clusters with multiple configurations, that with the lowest *gas-phase* potential energy was selected for the free energy calculations unless otherwise noted.

The hydration free energies for the clusters were determined using four variants of the integral-equation formalism polarizable continuum model (IEF-PCM),[2,61] which use different atomic radii to define the molecular cavity. These are (i) PCM_{UFF}, the Gaussian 09 default, which uses atomic radii from the Unified Force Field[62]; (ii) SMD, the model of Cramer, Truhlar, and co-workers,[63] which uses parametrized atomic radii or those from Bondi[64] for atoms not found in the large training set; (iii) PCM_{Bondi}, which uses atomic radii from Bondi[64] for all atoms—atomic radii for each model are tabulated in the Supporting Information, and the radii were scaled by 1.1 for both PCM_{UFF} and PCM_{Bondi}, which is done by default in Gaussian 09, and (iv) $PCM^{1.17}_{Bondi}$, for which the Bondi radii are scaled by a factor of 1.17, which yields radii similar to those used in COSMO.[4] The SMD model also includes nonelectrostatic contributions from an accessible surface area cavity-dispersion-solvent-structure term. Nonelectrostatic contributions were ignored for the other models.

All hydration free energy contributions were computed using either B3PW91 or B3LYP with the standard Pople basis set 6-311++G(d,p) for nonmetal atoms and the SDD basis set and pseudopotentials for the metal atoms.[65] Hydration contributions calculated with B3LYP are included as Supporting Information. For brevity, B3PW91 paired with the SDD/6-311++G(d,p) basis set is implied in the discussion of all solvent models, unless otherwise stated.

2.4. Cluster Configurations. For zero to six water molecules, the divalent metal cation clusters were limited to those with direct water–metal interactions. Inspired by QCT studies,[8,9] this constraint is straightforward to implement for the metals, and it avoids deviations between gas-phase and solution-phase structures. In the gas phase, second shell water–water interactions can be stronger than direct metal–water interactions.[66] For example, the configuration of Cu^{2+} clustered with four coordinating water molecules and two second shell water molecules is more stable than the configuration with all six water molecules interacting directly.[31] Using DFT, ref 31 found that this trend continues for eight and 10 water molecules but not 18, for which the configuration with six coordinated water molecules is more stable than the extended, planar configuration with four Cu^{2+}-coordinated water molecules. Similar observations are expected for Hg^{2+}, which is known to favor a 2-fold coordination environment.[67] Such configurational dependencies and phase deviations, while intrinsically interesting, are beyond the scope of the current investigation.

For clusters containing zero to six water molecules, locating stable geometries with direct anion–water interactions is less straightforward than for the metal cations. For anion–water molecule clusters, the configuration with the ion at the surface of the cluster can be more stable than that with the ion buried within.[12,14] For example, gas-phase clusters using 12 and 16 water molecules with F^- at the surface are 3–4 kcal mol^{-1} more stable than that where the F^- is tetrahedrally coordinated internal to the cluster.[14] The anions may be buried inside larger clusters. For example, in ref 14, the tetrahedrally coordinated F^- within the 16 water molecule cluster was found to be 3–4 kcal mol^{-1} more stable than the surface ion when continuum contributions were included. Subsequent calculations found that 15 and 18 water molecules were required to bury the F^- and Cl^- anions within the cluster.[68] While burying ions within the cluster may appear intuitive, recent studies of the macroscopic air/water interface suggest that some ions preferentially reside at the surface.[69] Indeed, a molecular thermodynamic analysis of salt effects on surface tension predicts that the free energy difference between surface- and bulk-hydrated ions is on the order of 1 kcal mol^{-1}, which may

dx.doi.org/10.1021/ct300296k | J. Chem. Theory Comput. XXXX, XXX, XXX–XXX

Table 1. Summary of Configurations and Thermal Contributions[a,b,c,d]

MP2/CBS	W_2	W_3	W_4	W_5	W_6	W_8[e]	W_{10}[e]
H_2O	2 (0.14)	3 (0.22)	6 (0.44)	8 (0.35)	6 (0.31)	3 (0.02)	2 (0.06)
OH^-	2 (0.00)	4 (0.14)	5 (0.30)	2 (0.15)	1 (0.00)	1 (0.00)	
SH^-	2 (0.03)	3 (0.06)	3 (0.17)	1 (0.00)	1 (0.00)	1 (0.00)	
Cl^-	3 (0.06)	3 (0.16)	8 (0.45)	3 (0.18)	3 (0.09)	1 (0.00)	
F^-	1 (0.00)	2 (0.06)	6 (0.40)	1 (0.00)	1 (0.00)	1 (0.00)	
Cu^{2+}	1 (0.00)	1 (0.00)	1 (0.00)	1 (0.00)	1 (0.00)		3 (0.09)
Zn^{2+}	1 (0.00)	1 (0.00)	1 (0.00)	1 (0.00)	1 (0.00)		2 (0.16)
Cd^{2+}	1 (0.00)	1 (0.00)	1 (0.00)	1 (0.00)	1 (0.00)		3 (0.09)
Hg^{2+}	1 (0.00)	1 (0.00)	1 (0.00)	1 (0.00)	1 (0.00)		2 (0.07)
B3PW91-D/*a*TZ	W_2	W_3	W_4	W_5	W_6	W_8	W_{10}
H_2O	2 (0.13)	3 (0.24)	6 (0.45)	8 (0.30)	6 (0.35)	3 (0.04)	2 (0.03)
OH^-	2 (0.02)	4 (0.12)	5 (0.33)	2 (0.15)	1 (0.00)	1 (0.00)	
SH^-	2 (0.08)	3 (0.18)	3 (0.14)	1 (0.00)	1 (0.00)	1 (0.00)	
Cl^-	3 (0.07)	3 (0.19)	8 (0.44)	3 (0.19)	3 (0.09)	1 (0.00)	
F^-	1 (0.00)	2 (0.08)	6 (0.37)	1 (0.00)	1 (0.00)	1 (0.00)	
Cu^{2+}	1 (0.00)	1 (0.00)	1 (0.00)	1 (0.00)	1 (0.00)		3 (0.01)
Zn^{2+}	1 (0.00)	1 (0.00)	1 (0.00)	1 (0.00)	1 (0.00)		2 (0.12)
Cd^{2+}	1 (0.00)	1 (0.00)	1 (0.00)	1 (0.00)	1 (0.00)		3 (0.14)
Hg^{2+}	1 (0.00)	1 (0.00)	1 (0.00)	1 (0.00)	1 (0.00)		2 (0.02)

[a]The integers denote the number of configurations. Thermal contributions in kcal mol^{-1} calculated as in ref 57 are in parentheses. Thermal contributions were not included in the hydration free energy calculations. Rather, the gas phase minima were used at each level of theory. [b]Standard rigid-rotor harmonic oscillator contributions included with scaled frequencies and simplified anharmonic corrections, see Theoretical Background and Methods. [c]Configurations (see Supporting Material) were chosen based on the minimum total potential energy at either the MP2/*a*TZ or B3PW91-D/*a*TZ level of theory. The two methods agreed on the minimum configuration for all species except the six-water cluster (see Figure 1). [d]A YAML file included in the Supporting Information contains all configurations and frequencies of clusters used in this study (136) along with all gas phase and continuum single-point calculations carried out with Gaussian 09. [e]See Figures 1−3 and the Supporting Information for structures.

be favorable or unfavorable depending on whether the ion is accumulated at or excluded from the surface.[70] In the present study, while the configurations of anions clustered with one to four water molecules should be sufficiently enumerated, the sampling of anions clustered with five and six water molecules was limited. Rather than extend the search for configurations, we take advantage of structurally similar surface ion clusters containing eight water molecules initiated from previous high-level ab initio studies.[12,14]

3. RESULTS AND DISCUSSION

In the following sections, we analyze the calculations of different legs of Scheme 1 performed with varying numbers of explicit water molecules and the polarizable continuum model (atomic radii for SMD, PCM_{Bondi}, and PCM_{UFF} are listed in Table S1). The hydration free energies of the divalent metal cations (Cu^{2+}, Zn^{2+}, Cd^{2+}, and Hg^{2+}) and anions (OH^-, SH^-, Cl^-, and F^-) are compared to experimental data and previous theoretical studies, where available. Hydration of the divalent metal cations is considered first, followed by the anions. Throughout, the accord between experiment and theory is assessed in terms of absolute and relative agreement.

All configurations considered in this study are included as Supporting Information, and a summary thereof is tabulated in Table 1. Deviations from minimum energy due to thermal configurational averaging are also tabulated in Table 1, for which contributions were on the order of 0.2 to 0.5 kcal mol^{-1} and were not included. The thermal configuration contributions and selection of the minimum energy structure are discussed further below for the six water cluster, which was the only set of configurations, in this study, for which MP2 and B3PW91-D have different minimum energy structures. Throughout this study, as mentioned in the methods, the configuration with the lowest gas-phase potential energy was used for all gas-phase and solution phase terms. The configurations for all ions clustered with one to six water molecules with the lowest MP2/CBS potential energy are displayed in Figures S1 to S8 of the Supporting Information.

For each set of solutes, comparisons between experiment and theory are carried out systematically with regard to Scheme 1 to contrast local and long-range hydration contributions.[71]

3.1. Water Clusters. *3.1.1. Hydration Free Energy of a Single Water Molecule.* The hydration free energy difference (referred to as the "residual error") between $\Delta G^*_{solv}((H_2O)_n)$ and $n\Delta G^*_{solv}(H_2O)$, including standard state contributions, was used in ref 17 to compare three continuum models. They found the residual error to be smallest for the COSMO hydration model, for which the self-hydration of a single water molecule (−6.7 kcal mol^{-1}) was close to the experimental value (−6.32 kcal mol^{-1}). The other two models (SM6[72] and a Poisson−Boltzmann method implemented in Jaguar[73]) overestimated the hydration of a water molecule by ∼2.5 kcal mol^{-1}. Here, the calculated hydration free energies of a single water molecule using SMD, PCM_{Bondi}, $PCM^{1.17}_{Bondi}$, and PCM_{UFF} were −8.5, −7.9, −6.7, and −5.0 kcal mol^{-1}, respectively. $PCM^{1.17}_{Bondi}$ agrees well with the experimental value of −6.32 kcal mol^{-1},[74] but the residual errors calculated using PCM_{UFF} are generally smaller (Table S13). To simplify the discussion, we focus primarily on continuum contributions from SMD and $PCM^{1.17}_{Bondi}$. Additional results for PCM_{Bondi} and PCM_{UFF} are included as Supporting Information.

3.1.2. Hydration Free Energy Differences Arising from Multiple Configurations of the Six Water Molecule Clusters. For all water and ion−water clusters in the current study, the configurations of the six water molecule clusters were the only case where the minimum energy structure differed between

dx.doi.org/10.1021/ct300296k | J. Chem. Theory Comput. XXXX, XXX, XXX−XXX

B3PW91-D/*a*TZ and MP2/CBS (see Figure 1). The minimum energy configuration for B3PW91/*a*TZ is the cyclic structure

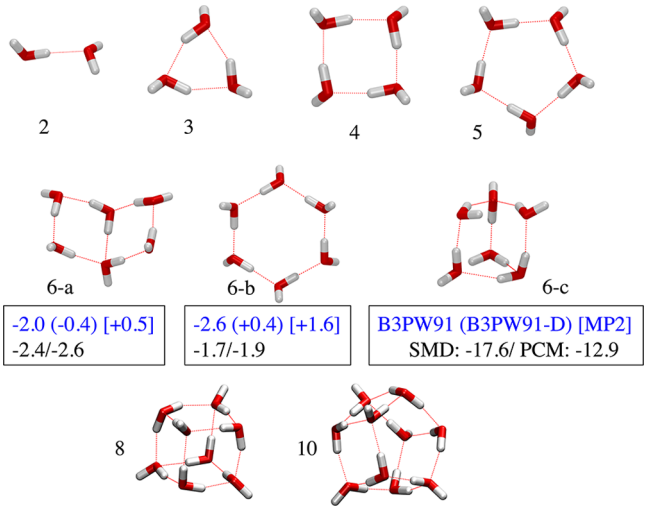

Figure 1. Gas-phase structures of water molecule clusters containing two to six, eight, and 10 water molecules. The multiple configurations of the six-water cluster correspond to the minimum potential energy configurations for B3PW91/*a*TZ, B3PW91-D/*a*TZ, and MP2/CBS, respectively, from left to right. For the six water cluster, adding the rigid-rotor harmonic vibrational contributions (with anharmonicity corrections) increases the stability of 6-a and 6-b by −0.4 and −1.5, respectively, relative to 6-c.

(6-b). Adding dispersion corrections, B3PW91-D/*a*TZ favors the book configuration (6-a) by 0.8 kcal mol^{-1} compared to the cyclic configuration and by 0.4 kcal mol^{-1} compared to the prism structure (6-c). The MP2/CBS level of theory predicts the prism structure (6-c) to be 1.6 and 0.5 kcal mol^{-1} more stable than either the ring or book configurations, respectively.[75]

As mentioned in the Theoretical Background and Methods, the contribution from the water clusters cancels for hydration free energy differences between clusters with the same number of explicit water molecules, for which the STDEVs are independent. On the other hand, the absolute values will change according to the combined gas-phase energy and bulk contributions. For example, swapping configuration 6-c with 6-b decreases the hydration free energies for each ion by 5.8 kcal mol^{-1} for B3PW91 and 2.8 (1.6) kcal mol^{-1} for B3PW91-D/*a*TZ (MP2/CBS) using SMD for bulk contributions. Thus, while the deviation from the minimum energy due to configurational averaging is relatively small, selecting the appropriate configuration is important when approximating the condensed-phase structure with that from the gas phase. While configurational averaging reduces the complexity of the bookkeeping for large collections of calculations such as the present case, we use the single minimum energy gas-phase structure to simplify discussions and aid analyses below. Future studies may benefit from the thermal averaging of sufficient numbers of conformers in both the gas and condensed phases, which effectively automates the selection of minimum energy configurations. Such an approach was used recently in the successful calculation of acid dissociation constants of dicarboxylic acids with zero to four explicit water molecules.[23]

3.2. Divalent Metal Cations M^{2+} = Cu^{2+}, Zn^{2+}, Cd^{2+}, and Hg^{2+}. *3.2.1. Gas-Phase Microsolvation: $\Delta G^{\circ}_{cluster}(W_n{\cdot}M^{2+})$.* Comparing the gas-phase cluster formation free energies to the experimental hydration free energies, the error decreases monotonically with an increasing number of explicit water molecules (Figure 4). At the B3PW91-D/*a*TZ level, when the number of explicit water molecules is increased from one to four, the MSE is reduced from −379.6 to −228.7 kcal mol^{-1}, and the STDEV decreases from 22.0 to 1.0 kcal mol^{-1}. Using six explicit water molecules increases the STDEV slightly to 1.2 kcal mol^{-1} and reduces the MSE further to −195.4. There are no standard state corrections included for the MSE at this stage. The corresponding trends for MP2/CBS

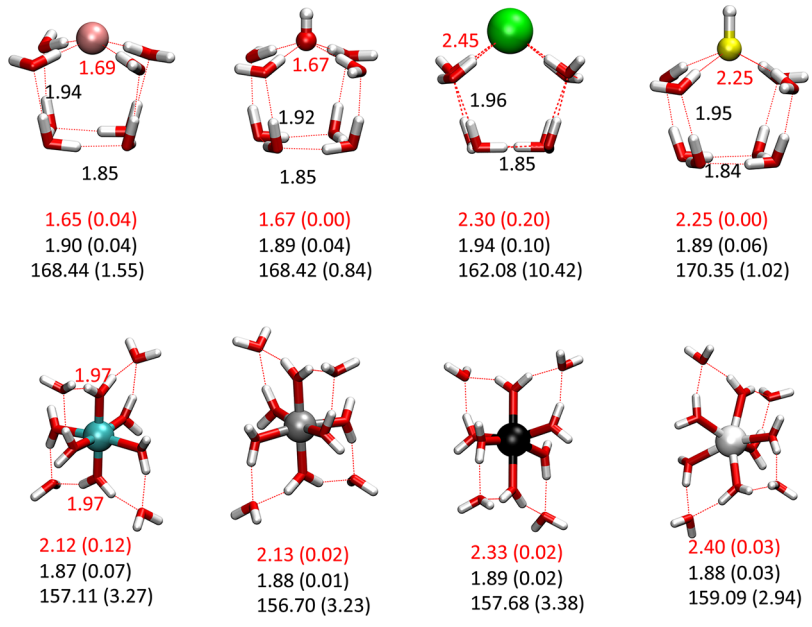

Figure 2. Gas-phase structures of the anions clustered with eight water molecules and the divalent metal cations clustered with 10 water molecules. Below each structure, the average (standard deviation) distances for the water−solute interactions are shown in red; the average (standard deviation) distances and angles corresponding to hydrogen bonds are shown below each cluster in black.

dx.doi.org/10.1021/ct300296k | *J. Chem. Theory Comput.* XXXX, XXX, XXX−XXX

are similar, but the errors are larger (Figure 4). Using four explicit water molecules, the MSE is −232.4 kcal mol^{-1}, and the STDEV is 3.3 kcal mol^{-1}. Using six water molecules, the STDEV increases to 4.3 kcal mol^{-1}, and the MSE is around 1 kcal mol^{-1} greater than that of B3PW91-D/*a*TZ.

The individual theoretical gas-phase cluster free energies for B3PW91-D and MP2 computed using various basis sets are tabulated in Table S8 of the Supporting Information and are briefly described here. As expected, B3PW91-D is not as sensitive to basis set choice as MP2. The hydration free energies typically differ by 0.5 kcal mol^{-1} upon increasing the basis set from *a*TZ to *a*QZ. In contrast, Cu^{2+}, Zn^{2+}, and Cd^{2+} gain around −3.5 kcal mol^{-1} for four to six water molecules while Hg^{2+} gains between −0.5 to −1.0 kcal mol^{-1} upon increasing the basis set from *a*TZ to the estimated CBS limit. These basis set contributions reduce the STDEV by ∼1 kcal mol^{-1} for MP2. B3PW91-D and MP2/CBS agree well (MP2/CBS is 1−2 kcal mol^{-1} more negative) for Cd^{2+} and Hg^{2+} clustered with four to six water molecules. In contrast, the agreement for Cu^{2+} and Zn^{2+} was not as good. The B3PW91-D free energies are more negative than the MP2/CBS by around 7−9 kcal mol^{-1} for Cu^{2+} and 3.5−4 kcal mol^{-1} for Zn^{2+} for forming clusters of four to six water molecules.

Using 10 water molecules (Figure 2), the STDEV for MP2/CBS decreases to 2.5 kcal mol^{-1} and increases for B3PW91-D/*a*TZ to 3.7 kcal mol^{-1}, indicating that the inclusion of second shell water molecules leads to improvements for MP2 and increased deviations from the experimental trends for B3PW91-D. These second shell effects highlight fortuitous error cancellation for DFT for smaller clusters. Using the 5-fold coordinated water configuration of Cu^{2+} (10-c in Figure 3) yields improved agreement with the experimental trends compared to the 6-fold coordinated configuration (10-a in Figure 3). Swapping the configuration 10-c with 10-a for Cu^{2+} (Figure 3) increases the STDEV by 1.6 kcal mol^{-1} for MP2/*a*TZ. The agreement with experimental values is improved further if the lower energy configuration (10-d) from ref 31 is used, for which adding −3.1 kcal mol^{-1} to the MP2/CBS energy calculated for configuration 10-c reduces the STDEV to 1.5 kcal mol^{-1}, which is in very good agreement with experimental trends.

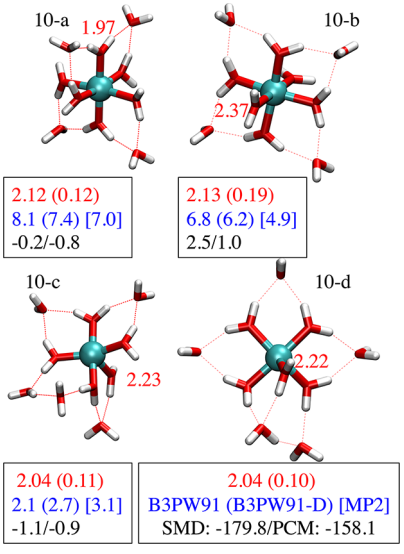

Figure 3. Gas-phase structures of the Cu^{2+} ions clustered with 10 water molecules. In the box below each structure, the average (standard deviation) Cu−O distance (Å) of coordinated water molecules is in red; the potential energy differences from configuration 10-d are in blue for B3PW91/*a*DZ, B3PW91-D/*a*DZ, and MP2/*a*TZ; the differences in free energy of the bulk contribution from SMD and $PCM^{1.17}_{Bondi}$, relative to 10-d, are in black. For 10-a and 10-b, the red number corresponds to the Cu−O distance (Å) of the two water molecules on opposite sides of the Cu atom (Figure 2). For 10-c and 10-d, the red number corresponds to the Cu−O distance (Å) of the axial water molecule. Configuration 10-d, from ref 31, is the most stable configuration.

The water−metal interaction strength decreases as the number of coordinated water molecules increases (Figure 5) and the gas-phase clusters approach configurations that are more representative of the solution. The Hg^{2+} ion is most interesting. The Hg^{2+}−water interaction strength is similar to Cu^{2+} and Zn^{2+} for two water molecules and becomes weaker and more similar to Cd^{2+} with additional water molecules. This observation is consistent with the prominence of 2-fold coordination environments for Hg^{2+},[67] which we discuss further below.

The improvement in relative trends between theory and experiment suggests that long-range contributions largely cancel and that the local interactions between the metal ion and the water molecules are sufficient when four, five, or six explicit water molecules are included. Improvements associated with extension to 10 water molecules highlight both the importance of second shell effects on charge distributions and the degree of intrinsic error associated with DFT, which varies for the different metals.

3.2.2. High-Level Corrections for Larger Water Clusters from Smaller Water Clusters. Here, we compare MP2/CBS calculations for divalent metal cations clustered with 10 water molecules to MP2/*a*TZ and B3PW91-D/*a*TZ with added corrections from smaller water clusters. Testing whether the basis set dependence of MP2 is dominated by the first hydration shell, the MP2/CBS limit for the larger system can be estimated as

$$\Delta G^{\circ}_{cluster}(10, \text{MP2/CBS}) \simeq \Delta G^{\circ}_{cluster}(10, \text{MP2/}a\text{TZ}) + [\Delta E_{cluster}(N_c, \text{MP2/CBS}) - \Delta E_{cluster}(N_c, \text{MP2/}a\text{TZ})] \quad (6)$$

where the bracketed terms on the right-hand side account for the difference in gas-phase cluster potential energy due to increasing the basis set from *a*TZ to CBS for the cluster with N_c water molecules. We use minimum energy structures for the smaller clusters in eq 6 and thus ignore basis set dependence of local structural deviations induced by the second shell. Using N_c = 5 for Cu^{2+} and N_c = 6 for the other ions yields basis set corrections of −3.2, −3.5, −3.6, and −0.5 kcal mol^{-1} for Cu^{2+}, Zn^{2+}, Cd^{2+}, and Hg^{2+}, respectively. Adding these basis set corrections to the MP2/*a*TZ values for clusters with 10 water molecules yields, in the same order, −342.2, −332.8, −281.7, and −285.9 kcal mol^{-1}, which are all slightly more positive (0.7, 0.4, 0.4, and 0.3 kcal mol^{-1}) than the full MP2/CBS results (Table S8). Making assumptions similar to eq 6, we can correct the DFT calculations of larger clusters. Adding a correction from B3PW91-D/*a*TZ to MP2/CBS for the smaller clusters (7.9, 3.6, −1.0, and −1.7 kcal mol^{-1} for Cu^{2+}, Zn^{2+}, Cd^{2+}, and Hg^{2+}) to B3PW91-D/*a*TZ yields, in the same order, −344.4, −332.5, −281.0, and −285.5 kcal mol^{-1}, which agree well with those from MP2/CBS. The more negative value for Cu^{2+}

dx.doi.org/10.1021/ct300296k | J. Chem. Theory Comput. XXXX, XXX, XXX−XXX

Table 2. Hydration Free Energies of the Divalent Metal Cations Calculated Using Gas-Phase Contributions from MP2/CBS or B3PW91-D/*a*TZ with Varying Numbers of Explicit Water Molecules (W) and Bulk Contributions from SMD or $PCM^{1.17}_{Bondi}$ at the B3PW91/6-311++G(d,p) Level of Theory[a]

species	W_0	W_1	W_2	W_3	W_4	W_5	W_6	W_{10}	VCC[b]
MP2/CBS		SMD							
Cu^{2+}	−473.9	−478.7	−472.4	−495.9	**−500.2**	−496.8	−497.3	−503.9	−489.1
Zn^{2+}	−476.0	−481.0	−487.7	**−494.6**	−495.3	−489.4	−489.2	−494.2	−486.5
Cd^{2+}	−420.1	−424.0	−427.8	**−435.4**	−437.9	−436.6	−439.6	−441.0	−427.2
Hg^{2+}	−435.8	−442.8	**−456.8**	−454.8	−451.4	−448.7	−449.9	−452.2	−455.0
STDEV	**9.0**	9.8	**18.2**	**7.9**	**4.6**	**4.8**	**5.4**	**3.3**	**11.1**
MSE	**−19.7**	**−14.5**	**−10.0**	**−1.0**	**0.1**	**−3.3**	**−2.2**	**1.7**	**−6.7**
MP2/CBS		$PCM^{1.17}_{Bondi}$							
Cu^{2+}	−401.3	−423.5	−433.1	−464.0	−476.1	**−476.7**	−480.6	−486.8	−468.7
Zn^{2+}	−404.1	−424.4	−444.9	−459.3	**−466.0**	−465.6	−471.0	−475.5	−458.6
Cd^{2+}	−355.7	−373.1	−389.2	−402.8	−410.0	−412.4	**−418.8**	−422.7	−402.9
Hg^{2+}	−364.4	−387.0	**−416.2**	−418.9	−420.0	−420.6	−424.4	−428.1	−415.1
STDEV	**10.4**	**9.7**	**17.5**	**6.0**	**1.6**	**1.5**	**2.1**	**1.1**	**2.7**
MSE	**−89.8**	**−69.2**	**−50.3**	**−34.9**	**−28.2**	**−27.3**	**−22.5**	**−17.9**	**−34.8**
B3PW91-D/*a*TZ		SMD							
Cu^{2+}	−473.9	−488.6	−486.4	−506.9	**−509.7**	−504.7	−501.6	−513.3	−498.3
Zn^{2+}	−476.0	−484.9	−493.2	−500.1	**−499.7**	−493.1	−489.6	−497.1	−491.1
Cd^{2+}	−420.1	−427.0	−431.9	−438.4	−439.1	−436.4	**−435.3**	−438.7	−429.9
Hg^{2+}	−435.8	−445.9	**−456.2**	−455.3	−451.0	−447.4	−444.9	−449.8	−454.1
STDEV	**9.0**	**7.2**	**12.4**	**4.6**	**2.6**	**1.6**	**1.4**	**3.2**	7.7
MSE	**−19.7**	**−9.6**	**−4.3**	**4.0**	**3.7**	**−0.8**	**−3.3**	**3.6**	**−2.8**
B3PW91-D/*a*TZ		$PCM^{1.17}_{Bondi}$							
Cu^{2+}	−401.4	−433.4	−447.1	−474.9	**−485.5**	−484.6	−484.8	−496.2	−477.9
Zn^{2+}	−404.1	−428.3	−450.4	−464.7	**−470.3**	−469.4	−471.2	−478.5	−462.7
Cd^{2+}	−355.7	−376.1	−393.4	−405.9	**−411.1**	−412.2	−414.5	−420.7	−403.5
Hg^{2+}	−364.4	−390.1	**−415.6**	−419.4	−419.6	−419.3	−419.4	−425.8	−414.2
STDEV	**10.8**	**6.8**	**11.6**	**2.8**	**3.4**	**2.7**	**2.5**	**4.7**	**3.2**
MSE	**−89.8**	**−64.2**	**−44.6**	**−29.9**	**−24.5**	**−24.8**	**−23.7**	**−15.9**	**−31.6**

[a]Experimental values (in kcal mol^{-1}) for Cu^{2+} (−505.9), Zn^{2+} (−493.5), Cd^{2+} (−439.1), and Hg^{2+} (−446.2) are from Fawcett. [b]VCC is calculated using the monomer thermodynamic cycle (see Theoretical Background and Methods). The numbers in boldface identify the locations of the VCC minima, and subtracting the two yields the difference in free energy due to changing of the thermodynamic cycles.

calculated with B3PW91-D suggests that deviations between DFT and MP2/CBS may extend to the second shell. The corrections should be further validated for larger clusters, for which small DFT errors in water−water interactions may accumulate. We expect such errors to largely cancel for relative trends as long as the numbers of water−water interactions are similar (Figure 6). Thus, such corrections are expected to improve relative trends predicted from calculations of larger clusters, for which MP2/CBS may be computationally prohibitive.

3.2.3. Continuum Contribution for Solvation of the Divalent Metal Cation−Water Clusters with Six or 10 Water Molecules, $\Delta G^*_{solv}(W_{n=6,10}\cdot M^{2+})$. The average (standard deviation) values for $\Delta G^*_{solv}(W_6\cdot M^{2+})$ are −208.6 (2.5) and −183.6 (2.3) kcal mol^{-1} for SMD and $PCM^{1.17}_{Bondi}$, respectively. Even with unfavorable contributions from nonelectrostatic terms, the average hydration free energy contribution for divalent metal cations from SMD is 25 kcal mol^{-1} more favorable, due largely to the smaller atomic radii. The individual SMD free energy contributions are −207.6, −207.7, −206.8, and −212.2 kcal mol^{-1} for Cu^{2+}, Zn^{2+}, Cd^{2+}, and Hg^{2+}, respectively. In contrast, the individual contributions, in the same order, for $PCM^{1.17}_{Bondi}$ are −186.2, −184.8, −181.4, and −182.1 kcal mol^{-1} and appear more in line with the expected trends from the experimental hydration free energies. As such, contributions from SMD will increase the hydration free energy of Hg^{2+} relative to the other divalent metal cations, and $PCM^{1.17}_{Bondi}$ will slightly increase the free energy gap between Cu^{2+}/Zn^{2+} and Cd^{2+}/Hg^{2+} pairs (Figure 5). However, overall, the continuum contributions are internally fairly similar, and thus the free energy trends predicted from the gas-phase cluster free energies alone should be robust. Using 10 explicit water molecules, the average (standard deviation) for $\Delta G^*_{solv}(W_{10}\cdot M^{2+})$ are −181.6 (3.0) and −157.3 (1.4) kcal mol^{-1} for SMD and $PCM^{1.17}_{Bondi}$, respectively, with similar trends discussed above for six explicit water molecules.

3.2.4. Summing up Contributions to $\Delta G^*_{solv}(M^{2+})$. Combining all terms from the cluster-continuum hydration free energy calculations using either a constant or variationally determined number of water molecules for each metal, we can compare absolute and relative agreement with experimental values. Using B3PW91-D and six explicit water molecules, the MSEs for SMD and $PCM^{1.17}_{Bondi}$ are −3.3 and −23.7 kcal mol^{-1}, respectively (Table 2). The corresponding STDEVs are 1.4 and 2.5 kcal mol^{-1}, which are in good agreement with the experimental free energy differences. Using gas-phase contributions from MP2/CBS with six explicit water molecules increases the STDEV to 5.4 kcal mol^{-1} for SMD and decreases slightly the STDEV for $PCM^{1.17}_{Bondi}$ to 2.1 kcal mol^{-1}. Using B3PW91-D and 10 explicit water molecules increases the STDEV to 3.2 and 4.7 for SMD and $PCM^{1.17}_{Bondi}$, in agreement with trends expected from the above analysis of errors in the

dx.doi.org/10.1021/ct300296k | J. Chem. Theory Comput. XXXX, XXX, XXX−XXX

gas-phase cluster free energies. Using MP2/CBS and 10 explicit water molecules improves the agreement with experimental values, for which the STDEV is 3.3 and 1.1 kcal mol^{-1} for SMD and PCM$^{1.17}_{\text{Bondi}}$, respectively. The corrections (assuming gas-phase thermal differences are negligible) associated with swapping the Cu^{2+} configuration 10-c for 10-d from ref 31 are −2.0 and −2.2 kcal mol^{-1} for SMD and PCM$^{1.17}_{\text{Bondi}}$, respectively (Figure 3). With the same correction for PCM$^{1.17}_{\text{Bondi}}$, the STDEV is reduced to 0.8 kcal mol^{-1}, which is in excellent agreement with experimental trends, and the MSE is −17.3 kcal mol^{-1}. With the same correction for SMD, the absolute values are −505.9, −494.2, and −441.0 kcal mol^{-1} for Cu^{2+}, Zn^{2+}, and Cd^{2+}, which are in excellent agreement with the experimental hydration free energies (see note a in Table 2).

As expected from the above discussion regarding SMD contributions, the hydration free energy of Hg^{2+} (−452.2 kcal mol^{-1}) is overestimated compared to the other metals and accounts for most of the STDEV (2.7) and MSE (2.1). For larger water clusters, we expect that the absolute agreement with experimental values will worsen for SMD, for which the hydration free energy will become overestimated, and improve for PCM$^{1.17}_{\text{Bondi}}$. On the other hand, the relative trends appear robust for either SMD or PCM$^{1.17}_{\text{Bondi}}$.

Using B3PW91-D/*a*TZ and 10 explicit water molecules with the MP2/CBS correction from smaller clusters discussed above, the agreement with experimental values is significantly improved. Adding the −1.6 and −1.8 kcal mol^{-1} corrections from swapping Cu^{2+} configuration (see Figure 3) 10-c for 10-d from ref 31 for SMD and PCM$^{1.17}_{\text{Bondi}}$, respectively, yields STDEVs (MSEs) of 2.4 (1.8) and 1.4 (−17.6) kcal mol^{-1}, which are in excellent agreement with those calculated using MP2/CBS.

Using MP2/CBS and PCM$^{1.17}_{\text{Bondi}}$, the free energy gained from increasing the coordination number and number of explicit water molecules differs greatly among the divalent metal ions (Figure 7). As mentioned above with respect to the gas-phase clustering free energies, the *n*-dependence of the hydration free energy of Hg^{2+} is quite interesting (Figure 5). Compared to the other divalent metal ions, Hg^{2+} interacts more strongly with fewer water molecules, and gains only −12 kcal mol^{-1} of free energy upon increasing the number of explicit water molecules from two to 10 (six of which directly coordinate). In contrast, in the same comparison, Cu^{2+} gains around −54 kcal mol^{-1} while Zn^{2+} and Cd^{2+} gain around −34 kcal mol^{-1}. Reflected in such hydration free energy trends is the ability of Hg^{2+} to interact strongly with biological molecules and compete with other metals for biologically important catalytic sites. Calculations of Hg^{2+} ligand binding free energies are being carried out and will be reported elsewhere.

3.2.5. The Variationally Determined Hydration Free Energy. In this section, we use MP2/CBS gas phase contributions (Table 2) for simplicity. As discussed in the Theoretical Background and Methods, the monomer cycle is used to determine the variational hydration free energies. See Figure S10 for plots comparing the two models and thermodynamic cycles discussed here. The variationally determined number of explicit water molecules depends on the particular thermodynamic cycle and polarizable continuum model. Using the monomer cycle reveals clear minima between one and six coordinated water molecules for both SMD and PCM$^{1.17}_{\text{Bondi}}$ (bold-faced numbers in Table 2). Using PCM$^{1.17}_{\text{Bondi}}$, the variational numbers of explicit water molecules are 5, 4, 6, and 2 for Cu^{2+}, Zn^{2+}, Cd^{2+}, and Hg^{2+}, respectively, and SMD shifts the coordination numbers down for all except Hg^{2+} (Table 2). In contrast, using the water cluster cycle (Scheme 1) generally shifts the minima in hydration free energy to those calculated using 10 water molecules (with exceptions for Zn^{2+} and Hg^{2+} only with SMD), a trend expected to continue with increasing *n*. Using PCM$^{1.17}_{\text{Bondi}}$ and the variationally determined number of explicit water molecules yields a STDEV of 2.7 kcal mol^{-1}, which is in reasonable agreement with experimental values. The much larger MSE (−34.8 kcal mol^{-1}), which is the highest value, reflects systematic errors associated with transferring *n* noninteracting water molecules from the continuum to a cluster with quantum mechanical interactions. Surveys of small molecule crystals show that the most common (second most common) coordination numbers for Cu^{2+}, Zn^{2+}, Cd^{2+}, and Hg^{2+} are 5 (4), 4 (6), 4 (6), and 2 (4),[67] respectively, which are in reasonable agreement with the variationally determined minima using MP2/CBS and PCM$^{1.17}_{\text{Bondi}}$. Along with the reduced error cancellation compared to the cluster cycle (Scheme 1), the monomer cycle (or a mixture of the two cycles) may still be an attractive and economical path for future development and validation of hydration methods where the sources of these errors may need to be investigated.

3.2.6. Comparison to a Previous Theoretical Study of Cu^{2+} Hydration. In agreement with results from a recent study of Cu^{2+} hydration,[17] the hydration free energies of divalent metal cations were found here to be underestimated when using six explicit water molecules. In that study, the hydration free energy of Cu^{2+} was calculated with six and 10 explicit water molecules to be −481.9 and −497.3 kcal mol^{-1}, respectively (Table 5 of ref 17) and was extrapolated via an 18 water molecule cluster to a best estimate of −509.0 kcal mol^{-1}, which is ∼3 kcal mol^{-1} more negative than the experimental value.[76] Using B3LYP/*a*TZ and PCM$^{1.17}_{\text{Bondi}}$ with six and 10 explicit water molecules, we obtained −480.7 and −494.5 kcal mol^{-1}, which are similar to those determined in ref 17.

The agreement with ref 17 using six explicit water molecules is slightly fortuitous and deserves further comment. The gas-phase cluster free energy calculated in ref 17 with B3LYP using rigid-rotor harmonic contributions corresponding to unscaled frequencies and a basis set similar to *a*TZ is −310.3 kcal mol^{-1}. Here, we obtain −304.3 kcal mol^{-1} with a similar level of theory and approximations. The majority of the 6.0 kcal mol^{-1} decrease in favorability calculated here is likely due to differences in the geometry of the Cu^{2+} water cluster. Ref 17 used Cu^{2+} with four directly coordinated water molecules and two in the second shell, and we used a configuration with six directly interacting water molecules. The agreement between hydration free energies is due to other terms. For example, 3.0 kcal mol^{-1} is regained from the difference in the continuum solvation (between the metal−water cluster and the water cluster), and 1.4 kcal mol^{-1} is from the approximate anharmonic corrections.

Similarly, using 10 explicit water molecules, the gas-phase cluster free energies are −351.0 and −355.0 kcal mol^{-1} calculated here and in ref 17, respectively. The main source of this difference in free energy is due to differences in the geometry of the Cu^{2+}−water cluster (Figure 3). Of the −4 kcal mol^{-1} deviation, −2.6 kcal mol^{-1} is accounted for by exchanging configurations 10-c and 10-d (Figure 3). The Cu^{2+} clustered with 10 water molecules reported here relaxed from an initial structure with six coordinated water molecules to a configuration with five (Figure 2). The difference in free energy from the continuum interactions with the metal−water

cluster and the water cluster is −140.2, which is only 0.5 kcal mol^{-1} more negative than that of ref 17. Our best estimate for the Cu^{2+}−10-water-molecule cluster (including MP2/*a*TZ corrections to configuration 10-d) using MP2/CBS gas-phase contributions paired with $PCM^{1.17}_{Bondi}$ is −489.0 kcal mol^{-1}, from which the hydration free energy calculated in ref 17 is likely overestimated by around 5−7 kcal mol^{-1} based on gas-phase clustering free energies calculated using MP2/CBS (Table S9).

3.3. Anions: OH^-, SH^-, Cl^-, and F^-. *3.3.1. Gas-Phase Microsolvation: $\Delta G^{\circ}_{cluster}(W_n{\cdot}L^-)$.* Similar to the treatment for divalent metal cations, the MSE and STDEV calculated from $\Delta G^{\circ}_{cluster}$ were found to improve with an increasing number of explicit water molecules (Figure 4). For the set of four anions,

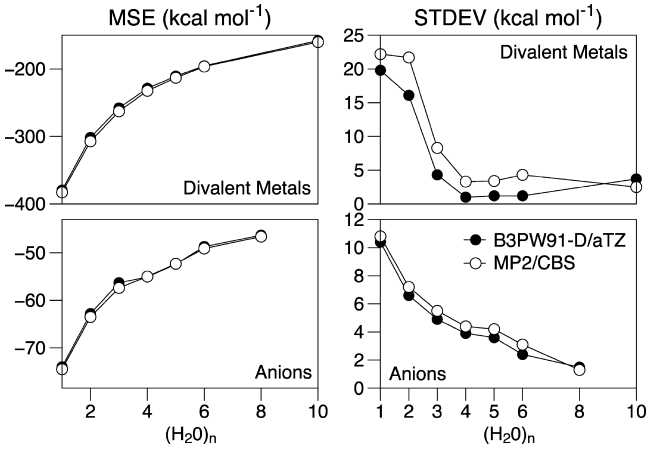

Figure 4. Comparisons between experimental hydration free energies and the theoretical gas-phase cluster free energies. The MSE (left column) and STDEV (right column) comparisons with experimental values are calculated using B3PW91-D/*a*TZ (filled circles) and MP2/CBS (open circles) for the set of divalent metal cations (Cu^{2+}, Zn^{2+}, Cd^{2+}, and Hg^{2+}) and anions (OH^-, SH^-, Cl^-, and F^-). See Tables S8 to S11 for the individual values and additional levels of theory.

as the size of the cluster is increased from one to six water molecules the MSE is decreased from −74.0 to −48.7 kcal mol^{-1} (Figure 4), and the STDEV of the average error is reduced from 10.4 kcal mol^{-1} to 2.4 kcal mol^{-1}. The STDEVs and MSEs with varying numbers of explicit water molecules agree very well between B3PW91-D/*a*TZ and MP2/CBS (Table S10). Compared to the divalent metal cations, gas-phase cluster free energies calculated at the B3PW91-D/*a*TZ level of theory, using five or six explicit water molecules is slightly less successful at predicting the experimental trends for the hydration free energies of anions (STDEV is ∼1 kcal mol^{-1} larger). The opposite is true for MP2/CBS where the STDEV for clustering divalent metals with six water molecules is around ∼1 kcal mol^{-1} larger than that of the anions. Clearly, differences in local interactions drive the hydration free energy differences, for which hydrogen bonds to either OH^- or F^- are much stronger than those to Cl^- or SH^- (Figure 5).

The individual theoretical gas-phase cluster free energies for DFT and MP2 computed with a series of basis sets are tabulated in Table S10 of the Supporting Information and are briefly described here. Compared to the divalent metal cations, MP2 is less sensitive to the size of the basis set. The free energies are typically within 0.5 kcal mol^{-1} upon increasing the basis set from *a*TZ to the estimated CBS limit. The agreement between B3PW91-D and MP2 is better (typically within 1−2

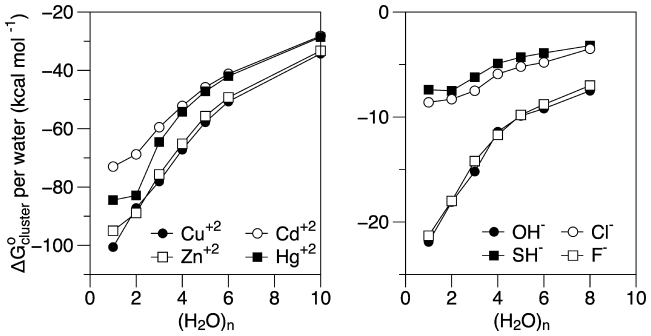

Figure 5. Free energies of forming the gas-phase clusters ($\Delta G^{\circ}_{cluster}$) calculated at the MP2/CBS level of theory normalized by the number of explicit water molecules for anions and divalent metal cations. As expected, the interaction strength per water molecule is reduced as the number of water molecules increases. The strengths of these local interactions clearly reflect the trends in hydration free energies. The Hg^{2+} ion is most interesting. The Hg^{2+}−water interaction strength is similar to Cu^{2+} and Zn^{2+} for two water molecules and becomes weaker and more similar to Cd^{2+} with additional water molecules.

kcal mol^{-1}) than that for the divalent metals. Thus, the anion hydration free energies calculated with gas-phase contributions from either level of theory are expected to be similar. More specifically, for two-water molecule clusters, B3PW91-D/*a*TZ deviates from MP2/CBS by −2.2, −0.4, +0.3, and −0.8 kcal mol^{-1} for OH^-, F^-, Cl^-, and SH^-, respectively, and by −2.0, +1.1, +1.5, and −0.9 kcal mol^{-1}, respectively, for eight-water molecule clusters. Using eight water molecules, the gas-phase contribution to the free energy difference between F^- and OH^- is 0.1 kcal mol^{-1} for MP2/CBS and around −3 kcal mol^{-1} for B3PW91-D/*a*TZ, for which the local interactions between the anion and water molecules are predicted to be relatively stronger for OH^- than F^-. Similarly, the difference between Cl^- and SH^- is −3.7 kcal mol^{-1} at the MP2/CBS level of theory and −1.3 kcal mol^{-1} at the B3PW91-D/*a*TZ level of theory. The experimental difference between Cl^- and SH^- is −2.4 kcal mol^{-1}.

The individual values obtained by clustering the anions with eight water molecules in the gas phase using MP2/CBS for OH^-, F^-, Cl^-, and SH^- are −56.9, −57.0, −29.6, and −25.9 kcal mol^{-1}, respectively. Using unscaled frequencies and conventional rigid-rotor harmonic vibrations approximations, the MP2/CBS values for OH^- and F^- are −58.9 and −59.3 kcal mol^{-1}, respectively, agreeing well with those calculated in refs 12 (−58.8) and 14 (−58.6) calculated with MP2/CBS approximated by extrapolations from *a*DZ, *a*TZ, and *a*QZ basis sets.

Using eight water molecules to calculate the gas-phase free energy of formation yields the best relative agreement with experimental results, for which the STDEVs (MSEs) are 1.3 (−46.5) and 1.3 (−46.2) kcal mol^{-1} for B3PW91-D/*a*TZ and MP2/CBS, respectively. The improved agreement with experimental values likely benefits energetically and structurally from the inclusion of second shell water molecules. The structural similarity is expected to facilitate error cancellation (Figure 6). Thus, for the sets of four divalent metal ions and four anions, the hydration free energy differences *within the sets* are reproduced well using only local interactions.

3.3.2. Continuum Contribution for Solvation of the Anion−Water Clusters with Two or Eight Water Molecules, $\Delta G^{*}_{solv} = (W_{m=2,8}{\cdot}L^-)$. The averages (standard deviations) of the continuum contributions for the anions clustered with two

dx.doi.org/10.1021/ct300296k | J. Chem. Theory Comput. XXXX, XXX, XXX−XXX

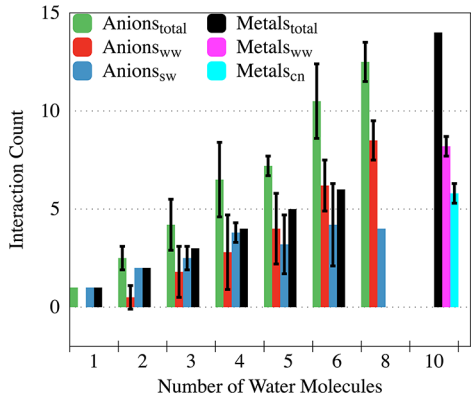

Figure 6. Comparisons of the total number of interactions involving water molecules for the divalent metal cations (black) and anions (green). The total number of interactions involving water molecules comprises the number of coordinated water molecules, solute−water (sw, shown for anions in blue) hydrogen bonds, and water−water (ww, shown for anions in red) hydrogen bonds. See notes for definitions.[98] The average number for each set is shown with an error bar that corresponds to plus or minus the standard deviation. For the divalent metal cations, each added water interacts only with the metal ion.

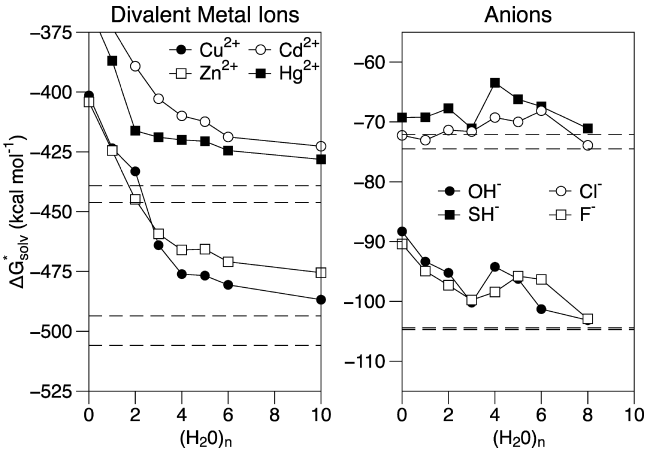

Figure 7. Hydration free energies of the anions and divalent metal cations calculated as a function of the number (n) of explicit water molecules using MP2/CBS for gas-phase contributions and $PCM^{1.17}_{Bondi}$ for contributions from bulk solvent. The experimental hydration free energies are shown with dashed lines. See Tables 2 and 3, note (a) for experimental hydration free energies.

water molecules are −65.9 (7.5) and −64.6 (4.6) kcal mol^{-1} for SMD and $PCM^{1.17}_{Bondi}$, respectively. The individual values of the SMD contribution are −73.6, −71.0, −60.2, and −58.8 kcal mol^{-1} for OH^-, F^-, Cl^-, and SH^-, respectively. These SMD contributions will increase the free energy gap between the two pairs of ions OH^-/F^- and Cl^-/SH^- (see Figure 5) by around 9 kcal mol^{-1} from those computed from gas-phase clustering. The averaged bulk solvent shifts ($\Delta G^*_{solv}(L^-\cdot W_2)-,\Delta G^*_{solv}(W_2)$, Scheme 1) for SMD and $PCM^{1.17}_{Bondi}$ are also similar because the increased favorability of the individual legs of SMD largely cancel. Subtracting the continuum contributions for W_2 reduces the averages to −51.9 and −53.6 kcal mol^{-1} for SMD and $PCM^{1.17}_{Bondi}$, respectively.

In contrast to using two water molecules, the average (standard deviation) continuum contributions for the anions clustered with eight water molecules are smaller at −61.8 (2.3) and −56.6 (0.9) kcal mol^{-1} for SMD and $PCM^{1.17}_{Bondi}$, respectively. The modest standard deviations in continuum contributions suggests that agreement with experimental trends achieved using gas-phase contributions for anions clustered with eight water molecules will be retained.

The bulk solvent shifts ($\Delta\Delta G^*_{solv} = \Delta G^*_{solv}(L^-\cdot W_8) - \Delta G^*_{solv}(W_8)$, see Scheme 1) are similar between SMD and $PCM^{1.17}_{Bondi}$ because the increased favorability of the individual legs of SMD largely cancels. The contributions from $\Delta G^*_{solv}(W_8)$ are −18.6 and −14.2 kcal mol^{-1} for SMD and $PCM^{1.17}_{Bondi}$, respectively. The individual values calculated using SMD are −45.0, −44.8, −40.2, and −42.6 kcal mol^{-1} for OH^-, F^-, Cl^-, and SH^-, respectively, and the same values calculated with $PCM^{1.17}_{Bondi}$ are −43.2, −42.9, −41.2, and −42.2 kcal mol^{-1}. The bulk solvent shifts for OH^- and F^- are slightly overestimated compared to refs 12 and 14, from which the values are −41.1 and −42.1 kcal mol^{-1}, respectively.

3.3.3. Summing up Contributions to $\Delta G^*_{solv}(L^-)$. The free energy differences are well reproduced using two water molecules with gas-phase contributions from the MP2/CBS level of theory paired with continuum contributions from SMD, the STDEV being 0.5 kcal mol^{-1}. Calculations with continuum contributions from $PCM^{1.17}_{Bondi}$ using two explicit water molecules are not as successful at reproducing free energy differences as those with SMD. The absolute hydration free energies are underestimated by around 7 kcal mol^{-1} using two water molecules with either SMD or $PCM^{1.17}_{Bondi}$ (Table 3). Using five explicit water molecules also yields underestimated hydration free energies with reasonable agreement with experimental trends, which may reflect fortuitous cancellation of error due to reduced structural variation (Figure 6). The STDEVs for VCC are not as successful as using two explicit water molecules but nevertheless yield reasonable values (Table 3).

Overall, using eight explicit water molecules with the MP2/CBS level of theory achieved the best absolute and relative agreement with experimental values using either SMD or $PCM^{1.17}_{Bondi}$, for which the STDEVs are 0.5 and 1.0 kcal mol^{-1}, respectively. The absolute hydration free energies calculated using eight water molecules at the MP2/CBS level of theory agree well with experimental values for both SMD and $PCM^{1.17}_{Bondi}$, for which the MSEs are −0.4 and −1.2 kcal mol^{-1}, respectively. Using MP2/CBS, the hydration free energies for OH^- and F^- are a few kilocalories per mole more negative than those determined in ref 12 (−101.0 kcal mol^{-1}) and ref 14 (−101.8 kcal mol^{-1}), largely due to differences in the treatment of the continuum contributions.[77] Using additional corrections from CCSD(T) and larger clusters, refs 12 and 14 were able to achieve excellent agreement with the absolute hydration free energies.

3.3.4. Comparison to Previous Theoretical Studies. Comparing the hydration of anions clustered with zero to six water molecules, the magnitudes of the STDEV and the MSE discussed above are not unreasonable with respect to previous studies.[10,17,18,63] For example, the SMD Coulombic radii, which depend only on atomic number and atomic surface tension parameters associated with nonelectrostatic contribution, were parametrized using a training set of 2821 solvation data points containing ions and neutral molecules in several solvents.[63] Therefore, it is not surprising that the small set of ions studied here with smaller numbers of water molecules would have MSEs on the order of −5 to −10 kcal mol^{-1}. Further, the experimental hydration free energies of cations and anions have been estimated to have errors of around ±2−3 kcal mol^{-1},[18,72]

dx.doi.org/10.1021/ct300296k | J. Chem. Theory Comput. XXXX, XXX, XXX−XXX

Table 3. Hydration Free Energies of the Anions Calculated Using Gas-Phase Contributions from MP2/CBS or B3PW91-D/*a*TZ with Varying Numbers of Explicit Water Molecules (W) and Bulk Contributions from SMD or $PCM^{1.17}_{Bondi}$ at the B3PW91/6-311++G(d,p) Level of Theory[a]

species	W_0	W_1	W_2	W_3	W_4	W_5	W_6	W_8	VCC[b]
MP2/CBS		SMD							
OH^-	−95.8	**−97.3**	−97.4	−101.8	−96.4	−97.7	−102.2	−105.0	−97.3
SH^-	−62.9	**−64.2**	−63.6	−67.7	−60.0	−63.9	−65.5	−71.5	−64.2
Cl^-	−65.6	**−67.8**	−67.1	−68.6	−66.8	−69.4	−68.9	−72.8	−67.8
F^-	−88.3	−93.5	**−96.4**	−98.6	−99.1	−98.3	−99.6	−104.8	−94.7
STDEV	**3.5**	**1.9**	**0.5**	**1.4**	**2.8**	**1.3**	**1.8**	**1.0**	**1.3**
MSE	**−10.8**	**−8.2**	**−7.8**	**−4.8**	**−8.3**	**−6.6**	**−4.9**	**−0.4**	**−7.9**
MP2/CBS[c]		$PCM^{1.17}_{Bondi}$							
OH^-	−88.3	−93.3	−95.2	**−100.2**	−94.2	−96.2	−101.3	−103.1	−94.2
SH^-	−69.3	**−69.2**	−67.7	−71.1	−63.5	−66.2	−67.4	−71.1	−69.3
Cl^-	−72.3	**−73.1**	−71.4	−71.6	−69.3	−70.0	−68.1	−73.9	−73.1
F^-	−90.4	−94.9	**−97.3**	−99.8	−98.4	−95.8	−96.3	−102.9	−96.2
STDEV	**7.4**	**4.9**	**2.8**	**1.7**	**2.4**	**2.0**	**2.0**	**0.5**	**4.3**
MSE	**−8.9**	**−6.3**	**−6.0**	**−3.3**	**−7.6**	**−6.9**	**−5.6**	**−1.2**	**−5.7**
B3PW91-D/*a*TZ		SMD							
OH^-	−95.8	**−99.0**	−99.6	−104.4	−97.1	−99.6	−101.8	−107.0	−99.0
SH^-	−62.9	**−64.6**	−64.4	−69.0	−60.1	−64.2	−63.0	−72.4	−64.6
Cl^-	−65.6	**−67.6**	−66.7	−68.4	−66.0	−68.5	−64.9	−71.3	−67.6
F^-	−88.3	−93.8	**−96.8**	−99.3	−98.9	−96.7	−95.4	−104.0	−94.8
STDEV	**3.5**	**2.1**	**1.3**	**2.6**	**2.7**	**1.4**	**3.2**	**2.3**	**1.7**
MSE	**−10.8**	**−7.7**	**−7.0**	**−3.7**	**−8.4**	**−6.7**	**−7.7**	**−0.3**	**−7.4**
B3PW91-D/*a*TZ		$PCM^{1.17}_{Bondi}$							
OH^-	−88.3	−95.0	−97.4	**−102.9**	−94.9	−98.2	−100.8	−105.1	−96.0
SH^-	−69.3	**−69.6**	−68.5	−72.3	−63.6	−66.5	−64.9	−72.0	−69.6
Cl^-	−72.3	**−72.8**	−71.0	−71.4	−68.4	−69.1	−64.1	−72.4	−72.8
F^-	−90.4	−95.2	−97.7	**−100.4**	−98.2	−94.2	−92.0	−102.0	−96.3
STDEV	**7.4**	**4.2**	**2.0**	**1.8**	**1.8**	**2.2**	**3.7**	**1.4**	**3.7**
MSE	**−8.9**	**−5.8**	**−5.3**	**−2.2**	**−7.6**	**−6.9**	**−8.5**	**−1.1**	**−5.3**

[a]Experimental values (in kcal mol^{-1}) for OH^- (−104.7), SH^- (−72.1), Cl^- (−74.5), and F^- (−104.4) are from Kelly et al.[15] Refs 15 and 25 are consistent for Cl^- and F^-. [b]VCC was calculated using the monomer thermodynamic cycle (see Theoretical Background and Methods). The numbers in boldface identify the locations of the VCC minima, and subtracting the two yields the difference in free energy due to changing the thermodynamic cycles.

although, the experimental errors are expected to be much smaller for the mono- and diatomic anions studied here.[12,14,15,17,24−26] While, the tabulated experimental hydration free energies of divalent metal cations may vary by over 20 kcal mol^{-1}, values that are consistently determined should be relatively accurate. See recent detailed discussions about the absolute hydration free energies of the proton and Cu^{2+} in ref 17, several monovalent and divalent metal ions in ref 35, and UO_2^{2+} in ref 49.

In the recent cluster-continuum study that used five explicit water molecules, the calculated hydration free energies for a series of 60 monovalent ions were shifted by different average errors for cations (−2.41 kcal mol^{-1}) and anions (−5.60 kcal mol^{-1}), and thermal corrections from gas-phase vibrational analysis were not included.[18] In that study, an ensemble of starting configurations was used for the gas-phase geometry optimizations, and a similar approach may yield improvements for the anion clusters containing five and six explicit water molecules studied here. The original VCC study found a systematic underestimation of 8.7 kcal mol^{-1} for a set of 14 anions and cations.[10] In the present study, for clusters that yield reasonable STDEVs, we find systematic underestimations of solvation free energies of anions similar to those listed above.

3.3.5. Combining the Sets of Anions and Divalent Metal Cations. Combining the sets of anions and divalent metal cations is not trivial. SMD was the only model able to align the MSEs of the two sets, for which the hydration free energies range from −72.1 kcal mol^{-1} for SH^- to −505.9 kcal mol^{-1} for Cu^{2+}. The large MSE for the metal cations calculated using $PCM^{1.17}_{Bondi}$ significantly increases the STDEV for the entire set. Using SMD with MP2/CBS, our best estimate following the above analysis yields a STDEV of 2.3 kcal mol^{-1} and an MSE of 0.9 kcal mol^{-1} for the entire set. Using SMD with B3PW91-D/*a*TZ and MP2/CBS corrections from small metal cation−water clusters yields a STDEV of 2.4 kcal mol^{-1} and an MSE of 0.7, which is in very good agreement with that from MP2/CBS. Adding an ad hoc +5 kcal mol^{-1} correction to the hydration free energy of Hg^{2+}, which appears overestimated by SMD compared to other divalent metal cations, reduces the STDEV and MSE for MP2/CBS to 1.1 and 0.2 kcal mol^{-1}, respectively. Investigations of larger clusters are being carried out to determine whether the hydration free energy differences diverge for SMD and converge for $PCM^{1.17}_{Bondi}$.

Using B3PW91-D/*a*TZ and SMD with two and six explicit water molecules for anions and divalent metal ions, respectively, the STDEV is 2.3 and MSE is −5.2 kcal mol^{-1}. The very good agreement with experimental trends for this computationally economical option is due, in part, to fortuitous error cancellation for divalent metal cations detailed above. Nevertheless, when carefully applied, such limited approaches

dx.doi.org/10.1021/ct300296k | J. Chem. Theory Comput. XXXX, XXX, XXX−XXX

should provide valuable insights into how hydration effects modulate metal ligand binding.

4. IMPLICATIONS AND CONCLUSIONS

A detailed characterization of how metals are hydrated is a prerequisite to understanding their behavior in aquatic environments and in biological systems, for which detailed mechanisms of uptake and transformation are still largely unknown.[78] In the present study, the aqueous hydration free energies of the set of group 12 divalent metal ions (Zn^{2+}, Cd^{2+}, and Hg^{2+}) together with Cu^{2+} and anions relevant in aquatic environments (OH^-, SH^-, Cl^-, and F^-) were calculated using DFT and MP2 cluster-continuum models. The number of explicit water molecules to include was explored in detail with the aid of comparisons to experimental data.

Accurate treatments of local interactions in the gas phase yielded very good relative agreement between theory and experimental hydration free energy trends. The MP2/CBS level of theory achieved better agreement with experimental values than DFT. Errors in DFT for the divalent metal cations were identified and corrected using gas-phase clustering free energies of smaller ion−water clusters calculated with MP2/CBS. Being dominated by local coordination interactions, the corrections from smaller clusters yielded excellent agreement between B3PW91-D/*a*TZ and MP2/CBS for larger clusters. The agreement between MP2/CBS and B3PW91-D/*a*TZ for the anion gas-phase clustering free energy was good. Bulk continuum contributions were required to accurately calculate hydration free energies for the entire set of four anions and four divalent metals with values ranging widely from −72.1 kcal mol^{-1} for SH^- to −505.9 kcal mol^{-1} for Cu^{2+}, for which SMD was the only model able to successfully align the MSEs of each set.

Due to reduced error cancellation, the variational approach (VCC) is less successful in predicting the experimental trends than using a constant number of explicit water molecules. These considerations highlight potential sources of error for cluster-continuum investigations of processes occurring in more varied electrostatic environments (such as biological macromolecules) where differences in the number of explicit water molecules may be presumed on the basis of structural or steric considerations. We expect that methods providing more faithful representations of the condensed phase, often at the expense of being more complex and technically challenging, have the potential to provide more robust predictions with improved accuracy. Promising approaches include quasichemical theory using condensed-phase simulations,[79−86] the shells theory of solvation,[87] and the application of metadynamics techniques to compute ion coordination free energy landscapes.[88]

Clearly, any high-level theoretical calculations that depend on minimum energy structures should beware of potential pitfalls.[89] In the present study, configurational sampling was avoided for larger clusters by harnessing structural similarity. A bootstrapping strategy was used in conjunction with detailed comparisons to experimental values in an effort to improve the accuracy of the cluster-continuum calculations for SH^-, Cl^-, Zn^{2+}, Cd^{2+}, and Hg^{2+} based on the successes of previous studies on OH^-,[12] F^-,[14] and Cu^{2+}.[17,31] Interestingly, for the divalent metal cations, Cu^{2+} naturally fell out of line with the six coordinated group 12 divalent ions to attain a 5-fold coordination that improved the agreement with experimental values. For the anions, surface ions interacting with two stacks of four water molecules were used. For either set of ions, the structures determined in this study may not accurately reflect the condensed-phase structure. Rather, at a minimum, quantum chemical calculations carried out for the structures reported here accurately capture the differences in the strength of interactions between similar ions (anions or divalent metal ions) clustered with water molecules.

When using cluster-continuum models that employ gas-phase geometries, we recommend using, if possible, constant numbers of explicit waters that are able capture local differences present in the condensed phase. For the anions studied here, using two explicit water molecules and SMD was as successful at predicting relative trends as using eight explicit water molecules, although the latter was required to reproduce absolute hydration free energies. In both cases, there is structural similarity in the configurations of the water molecule clusters for different ions, trivially for two water molecules and by design for eight water molecules. Clustering the anions with three to six water molecules in the gas phase, with regard to geometry optimization only, inevitably leads to second shell water−water interactions that vary from ion to ion and thus increase relative error.

While clusters that include a larger number of water molecules are better able to reproduce absolute and relative trends, they may not always be straightforward to apply or necessary to gain fundamental understanding. Even slightly larger ions, such as aromatic acids, may prove challenging for approaches involving large water clusters. For such species, a carefully developed quantum-continuum model, such as SMD, along with a carefully selected number of explicit water molecules seems a reasonable approach for general applications.

On the basis of the relative accuracy of metal hydration free energies discussed above, it is expected that the relative binding free energies of different metals and ligands can be successfully pursued. The relative errors from the gas-phase reaction, $\Delta G_g^\circ(ML_1L_2)$, of metals (M) and ligands may introduce additional errors, which are important to characterize. Previous successful DFT studies of metal ion selectivity indicate that such errors are unlikely to render careful applications of cluster-continuum approaches inadequate.[35,43,90,91] More ambitious cluster-continuum investigations that include both divalent and monovalent metal cations (such as coinage metals) binding to biological molecules, as carried out recently in ref 35, are also expected to yield reasonable relative binding free energies as long as the MSEs of the sets of metals (separated by oxidation state) are reasonably well-aligned.

■ ASSOCIATED CONTENT

Supporting Information

Additional tables and figures referenced by the main text are included. Hydration free energies calculated using other levels of theory and models are included. All geometries and energies are included in a YAML file. This material is available free of charge via the Internet at http://pubs.acs.org.

■ AUTHOR INFORMATION

Corresponding Author

*E-mail: smithjc@ornl.gov.

Notes

The authors declare no competing financial interest.

■ ACKNOWLEDGMENTS

We thank the reviewers for helpful suggestions. This work was conducted as part of the mercury Scientific Focus Area research program at Oak Ridge National Laboratory (ORNL), which is sponsored by the Subsurface Biogeochemical Research Program, Office of Biological and Environmental Research, U.S. Department of Energy (DOE). ORNL is managed by UT-Battelle, LLC for U.S. DOE under contract DE-AC05-00OR22725. This research used resources of the National Energy Research Scientific Computing Center, which is supported by the Office of Science of the U.S. DOE under Contract No. DE-AC02-05CH11231.

■ REFERENCES

(1) Tomasi, J.; Mennucci, B.; Cammi, R. *Chem. Rev.* **2005**, *105*, 2999−3094.
(2) Miertus, S.; Scrocco, E.; Tomasi, J. *Chem. Phys.* **1981**, *55*, 117−129.
(3) Cossi, M.; Barone, V.; Cammi, R.; Tomasi, J. *Chem. Phys. Lett.* **1996**, *255*, 327−335.
(4) Klamt, A.; Schüürmann, G. *J. Chem. Soc., Perkins Trans.* **1993**, *2*, 799−805.
(5) Cramer, C. J.; Truhlar, D. G. *Acc. Chem. Res.* **2008**, 760−768.
(6) Tawa, G. J.; Topol, I. A.; Burt, S. K.; Caldwell, R. A.; Rashin, A. A. *J. Chem. Phys.* **1998**, *109*, 4852−4863.
(7) Mejías, J. A.; S., L. *J. Chem. Phys.* **2000**, *113*, 7306−7316.
(8) Pratt, L. R.; Rempe, S. B. *AIP Conf. Proc.* **1999**, *492*, 172−201.
(9) Rempe, S. B.; Pratt, L. R.; Hummer, G.; Kress, J. D.; Martin, R. L.; Redondo, A. *J. Am. Chem. Soc.* **2000**, *122*, 966.
(10) Pliego, J. R.; Riveros, J. M. *J. Phys. Chem. A* **2001**, *105*, 7241−7247.
(11) Zhan, C.-G.; Dixon, D. A. *J. Phys. Chem. A* **2001**, *105*, 11534−11540.
(12) Zhan, C.-G.; Dixon, D. A. *J. Phys. Chem. A* **2002**, *106*, 9737−9744.
(13) Grabowski, P.; Riccardi, D.; Gomez, M. A.; Asthagiri, D.; Pratt, L. R. *J. Phys. Chem. A* **2002**, *106*, 9145−9148.
(14) Zhan, C.-G.; Dixon, D. A. *J. Phys. Chem. A* **2004**, *108*, 2020−2029.
(15) Kelly, C. P.; Cramer, C. J.; Truhlar, D. G. *J. Phys. Chem. B* **2006**, *110*, 16066−81.
(16) Chamberlin, A. C.; Cramer, C. J.; Truhlar, D. G. *J. Phys. Chem. B* **2006**, *110*, 5665−75.
(17) Bryantsev, V. S.; Diallo, M. S.; Goddard, W. A., III. *J. Phys. Chem. B* **2008**, *112*, 9709−19.
(18) da Silva, E. F.; Svendsen, H. F.; Merz, K. M. *J. Phys. Chem. A* **2009**, *113*, 6404−9.
(19) Pliego, J. R.; Riveros, J. M. *J. Phys. Chem. A* **2002**, *106*, 7434−7439.
(20) Liptak, M. D.; Shields, G. C. *Int. J. Quantum Chem.* **2001**, *85*, 727−741.
(21) Kelly, C. P.; Cramer, C. J.; Truhlar, D. G. *J. Phys. Chem. A* **2006**, *110*, 2493−9.
(22) Ho, J.; Coote, M. L. *J. Chem. Theory Comput.* **2009**, *5*, 295−306.
(23) Marenich, A. V.; Ding, W.; Cramer, C. J.; Truhlar, D. G. *J. Phys. Chem. Lett.* **2012**, *3*, 1437−1442.
(24) Tissandier, M. D.; Cowen, K. A.; Feng, W. Y.; Gundlach, E.; Cohen, M. H.; Earhart, A. D.; Coe, J. V.; Tuttle, T. R. *J. Phys. Chem. A* **1998**, *102*, 7787−7794.
(25) Fawcett, W. R. *J. Phys. Chem. B* **1999**, *103*, 11181−11185.
(26) Camaioni, D. M.; Schwerdtfeger, C. A. *J. Phys. Chem. A* **2005**, *109*, 10795−10797.
(27) Zhan, C. G.; Dixon, D. A. *J. Phys. Chem. B* **2003**, *107*, 4403−4417.
(28) Stanbury, D. M. *Adv. Inorg. Chem.* **1989**, *33*, 69−138.
(29) LaViolette, R. A.; Pratt, L. R. *Mol. Phys.* **1998**, *84*, 909−915.
(30) For example, a sphere for monatomic ions or a superposition of three spheres for CO_2.[83]
(31) Bryantsev, V. S.; Diallo, M. S.; van Duin, A. C. T.; Goddard, W. A., III. *J. Phys. Chem. A* **2008**, *112*, 9104−12.
(32) Ben-Naim, A.; Marcus, Y. *J. Chem. Phys.* **1948**, *81*, 2016−2027.
(33) Shepler, B. C.; Wright, A. D.; Balabanov, N. B.; Peterson, K. A. *J. Phys. Chem. A* **2007**, *111*, 11342−11349.
(34) Mori, S.; Endoh, T.; Yaguchi, Y.; Shimizu, Y.; Kishi, T.; Tesuya, Y. K. *Theor. Chem. Acc.* **2011**, *130*, 279−297.
(35) Rao, L.; Cui, Q.; Xu, X. *J. Am. Chem. Soc.* **2010**, *132*, 18092−102.
(36) Frisch, M. J.; Trucks, G. W.; Schlegel, H. B.; Scuseria, G. E.; Robb, M. A.; Cheeseman, J. R.; Scalmani, G.; Barone, V.; Mennucci, B.; Petersson, G. A.; Nakatsuji, H.; Caricato, M.; Li, X.; Hratchian, H. P.; Izmaylov, A. F.; Bloino, J.; Zheng, G.; Sonnenberg, J. L.; Hada, M.; Ehara, M.;Toyota, K.; Fukuda, R.; Hasegawa, J.; Ishida, M.; Nakajima, T.; Honda, Y.; Kitao, O.; Nakai, H.; Vreven, T.; Montgomery, J. A., Jr.; Peralta, J. E.; Ogliaro, F.; Bearpark, M.; Heyd, J. J.; Brothers, E.; Kudin, K. N.; Staroverov, V. N.; Kobayashi, R.; Normand, J.; Raghavachari, K.; Rendell, A.; Burant, J. C.; Iyengar,S. S.; Tomasi, J.; Cossi, M.; Rega, N.; Millam, N. J.; Klene, M.; Knox, J. E.; Cross, J. B.; Bakken, V.; Adamo, C.; Jaramillo, J.; Gomperts, R.; Stratmann, R. E.; Yazyev, O.; Austin, A. J.; Cammi, R.; Pomelli, C.; Ochterski, J. W.; Martin, R. L.; Morokuma, K.; Zakrzewski, V. G.; Voth, G. A.; Salvador, P.; Dannenberg, J. J.; Dapprich, S.; Daniels, A. D.; Farkas, Ö.; Foresman, J. B.; Ortiz, J. V.; Cioslowski, J.; Fox, D. J. *Gaussian 09*, Revision A.1, Gaussian, Inc., Wallingford CT, 2009.
(37) Becke, A. D. *J. Chem. Phys.* **1993**, *98*, 5648−5652.
(38) Perdew, J. P.; Wang, Y. *Phys. Rev. B* **1992**, *45*, 13244−13249.
(39) Lee, C.; Yang, W.; Parr, R. G. *Phys. Rev. B* **1988**, *37*, 785−789.
(40) Stephens, P. J.; Devlin, F. J.; Chabalowski, C. F.; Frisch, M. J. *J. Phys. Chem.* **1994**, *98*, 11623−11627.
(41) Møller, C.; Plesset, M. S. *Phys. Rev.* **1934**, *46*, 618−622.
(42) Donald, K.; Hargittai, M.; Hoffmann, R. *Chem.—Eur. J.* **2009**, *15*, 158−177.
(43) Tai, H.-C.; Lim, C. *J. Phys. Chem. A* **2006**, *110*, 452−462 PMID: 16405317.
(44) Castro, L.; Dommergue, A.; Renard, A.; Ferrari, C.; Ramirez-Solis, A.; Maron, L. *Phys. Chem. Chem. Phys.* **2011**, *13*, 16772−9.
(45) Parks, J. M.; Guo, H.; Momany, C.; Liang, L.; Miller, S. M.; Summers, A. O.; Smith, J. C. *J. Am. Chem. Soc.* **2009**, *131*, 13278−85.
(46) Grimme, S.; Antony, J.; Ehrlich, S.; Krieg, H. *J. Chem. Phys.* **2010**, *132*, 154104.
(47) Grimme, S.; Ehrlich, S.; Goerigk, L. *J. Comput. Chem.* **2011**, *32*, 1456−1465.
(48) Temelso, B.; Shields, G. *J. Chem. Theory Comput.* **2011**, *7*, 2804−2817.
(49) Gutowski, K. E.; Dixon, D. A. *J. Phys. Chem. A* **2006**, *110*, 8840−8856.
(50) Yoo, S.; Apr'a, E.; Zeng, X. C.; Xantheas, S. S. *J. Phys. Chem. Lett.* **2010**, *1*, 3122−3127.
(51) Dunning, T., Jr.; Peterson, K.; Wilson, A. *J. Chem. Phys.* **2001**, *114*, 9244.
(52) Kendall, R.; Dunning, T., Jr.; Harrison, R. *J. Chem. Phys.* **1992**, *96*, 6796−6806.
(53) Andrae, D.; Haussermann, U.; Dolg, M.; Stoll, H.; Preuss, H. *Theor. Chim. Acta* **1991**, *78*, 247−266.
(54) Halkier, A.; Klopper, W.; Helgaker, T.; Jorgensen, P.; Taylor, P. R. *J. Chem. Phys.* **1999**, *111*, 9157−9167.
(55) Valiev, M.; Bylaska, E. J.; Govind, N.; Kowalski, K.; Straatsma, T. P.; van Dam, H. J. J.; Wang, D.; Nieplocha, J.; Apra, E.; Windus, T. L.; de Jong, W. A. *Comput. Phys. Commun.* **2010**, *181*, 1477−1489.
(56) Shields, R. M.; Temelso, B.; Archer, K. A.; Morrell, T. E.; Shields, G. C. *J. Phys. Chem. A* **2010**, *114*, 11725−11737.
(57) Temelso, B.; Archer, K. A.; Shields, G. C. *J. Phys. Chem. A* **2011**, *115*, 12034−12046.
(58) Pratt, L. M.; Truhlar, D. G.; Cramer, C. J.; Kass, S. R.; Thompson, J. D.; Xidos, J. D. *J. Org. Chem.* **2007**, *72*, 2962−2966.

(59) Zhao, Y.; Truhlar, D. G. *Phys. Chem. Chem. Phys.* **2008**, *10*, 2813−2818.
(60) Ribeiro, R. F.; Marenich, A. V.; Cramer, C. J.; Truhlar, D. G. *J. Phys. Chem. B* **2011**, *115*, 14556−14562.
(61) Mennucci, B.; Cancès, E.; Tomasi, J. *J. Phys. Chem. B* **1997**, *101*, 10506−10517.
(62) Rappe, A. K.; Casewit, C. J.; Colwell, K. S.; Goddard, W. A.; Skiff, W. M. *J. Am. Chem. Soc.* **1992**, *114*, 10024−10035.
(63) Marenich, A. V.; Cramer, C. J.; Truhlar, D. G. *J. Phys. Chem. B* **2009**, *113*, 6378−96.
(64) Bondi, A. *J. Phys. Chem.* **1964**, *68*, 441−451.
(65) Peterson, K. A.; Puzzarini, C. *Theor. Chim. Acta* **2005**, *114*, 283−296, DOI: 10.1007/s00214-005-0681-9.
(66) Stace, A. *Phys. Chem. Chem. Phys.* **2001**, *3*, 1935−1941.
(67) Dudev, M.; Wang, J.; Dudev, T.; Lim, C. *J. Phys. Chem. B* **2006**, *110*, 1889−95.
(68) Kemp, D. D.; Gordon, M. S. *J. Phys. Chem. A* **2005**, *109*, 7688−7699.
(69) Petersen, P. B.; Saykally, R. J. *Annu. Rev. Phys. Chem.* **2006**, *57*, 333−364.
(70) Pegram, L. M.; Record, M. T. *J. Phys. Chem. B* **2007**, *111*, 5411−5417.
(71) Clearly, local and long-range contributions are not entirely separable. Large gas-phase clusters will have some nonlocal interactions, and conversely, the hydration of small or anisotropic solute−water clusters with exposed solute surfaces will have local contributions from the continuum.
(72) Kelly, C. P.; Cramer, C. J.; Truhlar, D. G. *J. Chem. Theory Comput.* **2005**, *1*, 1133−1152.
(73) *Jaguar*, version 7.0; Schrödinger, LLC: New York, 2007.
(74) Afeefy, H.; Liebman, J.; Stein, S. In *NIST Chemistry WebBook, NIST Standard Reference Database Number 69*; Linstrom, P., Mallard, W., Eds.; National Institute of Standards and Technology: Gaithersburg MD. http://webbook.nist.gov (accessed Nov. 2012).
(75) The structure and energetics of water clusters have been discussed in impressive detail recently.[57] Even more recently, the cage configuration has been experimentally determined to be the global minimum for the cluster of six water molecules in the gas phase.[92] As mentioned in the Theoretical Background and Methods, the water cluster configurations taken from refs 56 and 57 were reoptimized with density functional theory to be consistent with all other clusters. Here, at the MP2/CBS level, the cage configuration was 0.03 kcal mol^{-1} less stable than the prism configuration. On the other hand, the contribution from SMD was ∼1.5 kcal mol^{-1} more favorable for the prism configuration, which highlights the challenges of predicting absolute hydration free energy values using cluster-continuum models using a single gas-phase minimum.
(76) In ref 17, the hydration free energy of Cu^{2+} was calculated with the B3LYP functional[37,39,40] and the COSMO[93] solvation model. Solvation contributions were calculated with the 6-311++G(d,p) basis set for oxygen and hydrogen atoms and the LACV3P pseudopotential[94] and basis for Cu. Gas-phase cluster free energy contributions were calculated at the B3LYP/LACV3P+/aug-cc-pVTZ(-f) level of theory.
(77) Concentration corrections were added here, see eq 3. Refs 12 and 14 used the surface and volume polarization for the electrostatic interaction method (SVPE)[95,96] at the HF/6-31++G** level of theory.
(78) Barkay, T.; Miller, S. M.; Summers, A. O. *FEMS Microbiol. Rev.* **2003**, *27*, 355−384.
(79) Asthagiri, D.; Pratt, L. R.; Kress, J. D. *Phys. Rev. E: Stat. Nonlin. Soft Matter Phys* **2003**, *68*, 041505.
(80) Asthagiri, D.; Pratt, L. R.; Kress, J. D.; Gomez, M. A. *Proc. Natl. Acad. Sci. U. S. A.* **2004**, *101*, 7229−33.
(81) Asthagiri, D.; Pratt, L. R.; Kress, J. D. *Proc. Natl. Acad. Sci. U. S. A.* **2005**, *102*, 6704−8.
(82) Chempath, S.; Pratt, L. R.; Paulaitis, M. E. *J. Chem. Phys.* **2009**, *130*, 054113.
(83) Jiao, D.; Rempe, S. B. *J. Chem. Phys.* **2011**, *134*, 224506.
(84) Rogers, D. M.; Beck, T. L. *J. Chem. Phys.* **2008**, *129*, 134505.
(85) Rogers, D. M.; Beck, T. L. *J. Chem. Phys.* **2010**, *132*, 014505.
(86) Merchant, S.; Dixit, P. D.; Dean, K. R.; Asthagiri, D. *J. Chem. Phys.* **2011**, *135*, 054505.
(87) Pliego, J. *Theor. Chim. Acta* **2011**, *128*, 275−283.
(88) Brancato, G.; Barone, V. *J. Phys. Chem. B* **2011**, *115*, 12875−12878.
(89) Yu, H.; Roux, B. *Biophys. J.* **2009**, *97*, L15−L17.
(90) Dudev, T.; Lim, C. *Ann. Rev. Biophys.* **2008**, *37*, 97−116.
(91) Dudev, T.; Lim, C. *J. Phys. Chem. B* **2009**, *113*, 11754−64.
(92) Pérez, C.; Muckle, M. T.; Zaleski, D. P.; Seifert, N. A.; Temelso, B.; Shields, G.; Kisiel, Z.; Pate, B. H. *Science* **2012**, *336*, 897−901.
(93) Klamt, A.; Schuurmann, G. *J. Chem. Soc., Perkin Trans. 2* **1993**, 799−805.
(94) Hay, P. J.; Wadt, W. R. *J. Chem. Phys.* **1985**, *82*, 299−310.
(95) Chipman, D. M. *J. Chem. Phys.* **1997**, *106*, 10194−10206.
(96) Zhan, C. G.; Bentley, J.; Chipman, D. M. *J. Chem. Phys.* **1998**, *108*, 177−192.
(97) Pyykko, P.; Atsumi, M. *Chem.—Eur. J.* **2009**, *15*, 186−197.
(98) Specification of interactions: A water is considered coordinated to a solute atom if the water oxygen is within a third of the sum of the combined covalent radii.[97] A hydrogen bond between two oxygens exists if they are within 3.5 Å and the angle about the shared hydrogen atom is ≥140°. A hydrogen bond between an oxygen and sulfur or chloride atom exists if the two atoms are within 3.8 Å and the angle about the shared hydrogen atom is ≥140°.